The suitability of gibbsite as aluminum source to complex with dissolved organic matter

In the interest of soil permeability reduction

M.K. Veerkamp

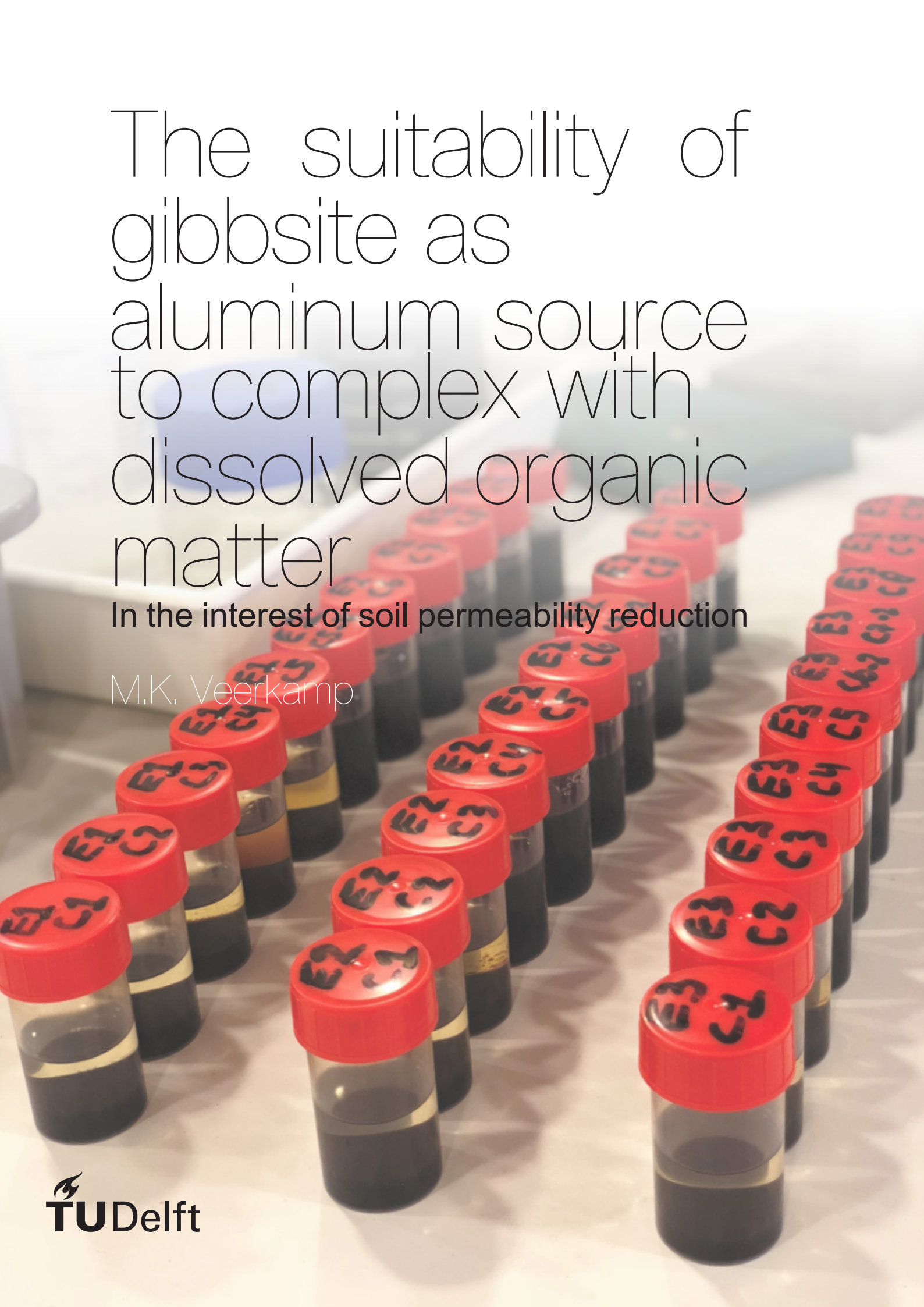

TU Delft

The suitability of gibbsite as aluminum source to complex with dissolved organic matter

In the interest of soil permeability reduction

by

M.K. Veerkamp

to obtain the degree of Master of Science
at the Delft University of Technology
to be defended publicly on Wednesday July 6th 2018 at 13:30.

Student number:	4522427	
Project duration:	October 2017 – July 2018	
Thesis committee:	prof. dr. ir. T.J. Heimovaara	TU Delft, Geo-Engineering
	ir. J. Zhou	TU Delft, Geo-Engineering
	dr. S.J. Laumann	TU Delft, Geo-Engineering
	dr. J. Gebert	TU Delft, Geo-Engineering
	dr. C. Chassagne	TU Delft, Environmental Fluid Mechanics

TU Delft

Preface

This Master thesis, ”The feasibility of gibbsite as aluminum source to complex with dissolved organic matter”, is the final requirement to obtain the degree of Master of Science for Geo-engineering, a master track in the Civil Engineering programme, at the faculty of Civil Engineering and Geosciences at Delft University of Technology. I conducted my research at Delft University of Technology from October 2017 to July 2018.

This research is part of the SoSEAL project, which is aiming at developing an engineering solution to reduce soil permeability in-situ. I was inspired by the concept of solving an engineering problem in an ecological friendly way.

This thesis could not have been realised without a few people who supported me during my research. First of all I want to thank my graduation committee: Timo Heimovaara, Julia Gebert, Susanne Laumann, Claire Chassagne and Jiani Zhou. I would like to voice my appreciation to Timo Heimovaara for his ideas and for giving me the confidence to tackle occurring problems. I especially like to express my gratitude to Jiani Zhou, my daily supervisor. His feedback has helped me a lot and I have enjoyed our numerous meetings. I could not have performed my experiments without the laboratory support of Jolanda van Haagen. Lastly I would like to thank my family, friends, room-mates and Loys for their support.

M.K. Veerkamp
Delft, July 2018

Summary

Controlling subsurface flow is crucial to prevent: the spreading of contaminants, the failure of dykes or any undesirable water flow. Subsurface flow can be controlled by changing the soil permeability. In order to change soil permeability rigid structures are often installed (for example the installation of sheet pile walls into dyke bodies), however, these solutions are costly and disrupts the environment. Alternatively, the SoSEAL project aims to provide an in-situ solution to reduce the permeability of highly permeable soil layers in an ecological friendly and cost-effective way. The SoSEAL project is inspired by podzolization, which is a soil formation process. It reduces soil permeability via the precipitation of metal-organic matter complexes in the pore space. During earlier practices a need has arisen for a cheap, environmentally friendly and naturally available aluminum source. Accordingly, the goal of this research is to investigate if gibbsite can be used as the aluminum source to form metal-organic matter precipitates.

A literature study was conducted to investigate the interplay between gibbsite and dissolved organic matter (DOM). Four processes are primarily studied in this research, they are: the release of free Al via dissolution of gibbsite; the complexation between free Al and DOM; the protonation and subsequently precipitation of DOM and the adsorption of H^{+}/DOM onto the gibbsite surface. Thereafter the following hypotheses were formulated:

- The extent of gibbsite dissolution is larger at low pH. However, due to its low solubility and slow dissolution kinetics, a low concentration of free Al is expected.
- The organic matter (OM) source used in this study is a humic acid, therefore it is expected to become completely insoluble when the pH is below two.
- The contradicting pH dependency of gibbsite dissolution and OM solubility leads a narrow transitional pH range, that is favourable for the occurrence of complexation between free Al and DOM.

These hypotheses are tested by performing experiments in the laboratory, where the pH varies from 2 to 8 and the aluminum/carbon (mol/mol) ratio is 0 ; 0.05; 0.1; 0.3 and 1. A synthesized crystalline gibbsite powder and a potassium humate is used.

The results are subdivided into three pH ranges in which similar behaviour was found. In the low pH range (pH = 2 - 2.5), the protonation and subsequently precipitation of DOM is the dominant process in short term. However, when considering the long term behaviour, gibbsite dissolution is the dominant process as the DOM has precipitated. Due to the difference in time scale, there is very little complexation between free Al and DOM. In the transitional pH range (pH = 3 - 3.5), the competition for H^{+} between DOM and gibbsite is profound. This increases the solubility of DOM and slows the dissolution of gibbsite down. As a consequence, this favours the gradual complexation between free Al and DOM. Nevertheless, due to ambiguity of the free Al measurement method used in this research, it is difficult to quantify the complexation. In neutral to high pH range (pH = 4 - 8) DOM undergoes protonation over time but stays soluble. The release of free Al via the dissolution of gibbsite is negligible in this pH range. Therefore complexation between free Al and DOM should not be expected.

The results presented in this research indicate that gibbsite may not be suitable as the aluminum source to form precipitates with organic matter in engineering solutions that require fast soil permeability reduction. However, the slow release of free Al from gibbsite in combination with the gradual formation of precipitates with organic matter might be interesting for robust problems that require a self healing ability. For efficiency concern, another OM source that is rich in fulvic acids (higher solubility at low pH than humic acid) and a natural gibbsite source (higher solubility than synthesized gibbsite) should be investigated.

Contents

Nomenclature

Abbreviations

SoSEAL	Soil Sealing by Enhanced Aluminum and DOM Leaching
Al	free Aluminum
DLM	Diffusive Layer Model
DOM	Dissolved Organic Matter
EC	Electrical Conductivity
FA	Fulvic Acid
G	amount of Gibbsite
H	Humin concentration
HA	Humic Acid
HMW	Heigh Molecular Weight
LMW	Low Molecular Weight
OM	Organic Matter
PPZC	Pristine Point of Zere Charge
PZNPC	Point of Zero Net Proton Charge
PZC	Point of Zere Charge
UV	Ultra Violet

Symobls

T	Temperature
K	Equilibrium constant
$\mathrm{K_{s,am}}$	Solubility constant amorphous gibbsite
$\mathrm{K_{s,cr}}$	Solubility constant crystalline gibbsite
$\equiv$	Surface
$\mathrm{K^{app}}$	Apparent equilibrium constant
$\mathrm{K^{int}}$	Intrinsic equilibrium constant
$\Delta \mathrm{Z}$	Change in charge
F	Faraday constant
Ψ	surface potential
R	Gas constant
VE	Electrical interaction energy
VA	Van der Waals interaction energy
VT	Total interaction energy
ϕ_e^i	Radiant flux received by DOM
ϕ_e^t	Radiant flux transmitted by DOM
Δ	Delta

List of Figures

List of Tables

1 Introduction

Permeability is a crucial characteristic of soil (Holtz, 1974). The permeability can be defined as the ability of a porous mass to allow passage of water through itself. A great deal of civil engineering problems have to do with soil permeability. The permeability can either be too low, in for example consolidation problems. In this case drains are often installed to lower the drainage path and subsequently reduce the consolidation time (Yong and Townsend, 1986). Or the permeability can be too high, for example in hydraulic problems as the pollution of ground- and drinking water by the spreading of contaminants or the intrusions of seawater (Uddameri et al., 2014). Another common high permeability problem is the seepage through dikes. By internal erosion of the dike this seepage can lead to dike instability (Xu, 2013). Existing techniques to lower soil permeability are based on the installation of rigid structures and therefore costly and radically, there is room for improvement.

Therefore a new idea of permeability reduction has been tested in the SoSEAL (Soil Sealing by Enhanced Aluminum and DOM Leaching) project. The aim of the SoSEAL project is to reduce the permeability of high permeable soil layers in-situ without much disruption of the above ground activities in a ecological friendly way. Furthermore, by being an in-situ method and using natural materials the technique also has the potential to be more cost-effective than existing techniques.

The SoSEAL concept is inspired by podzolization. Podzolization is a complex soil formation process in which metal ions and dissolved organic matter (DOM) form complexes and precipitate, occupying the pore space and thereby creating a low permeability layer (Lundström et al., 2000a). A more detailed description of the podzolization process is given in appendix A.

In podzols aluminum and iron are the crucial metal ions. These trivalent metal ions showed to bind stronger and be more effective in forming insoluble complexes with DOM then divalent or monovalent metal ions (Nierop et al., 2002; Weng, 2002). The reduced state of iron, Fe^{2+}, is less efficient in complexing with DOM than Fe^{3+} and Al^{3+} (Jansen et al., 2001), moreover Fe^{2+}-DOM complexes stay soluble (Nierop et al., 2002). Because organic matter (OM) can mediate the reduction of Fe^{3+} (Clarke and Danielsson, 1995) and Fe^{3+}-DOM complexes can be microbially reduced to the lesser stable Fe^{2+}-DOM complexes (Eusterhues et al., 2014), aluminum is used as metal ion source in the SoSEAL project.

Previous studies within the SoSEAL project have been carried out by Bonfiglo (2016); Hopman (2016); Popma (2017) and Vis (2015). Furthermore, one pilot project has been successfully finished (Laumann et al., 2016). Similarity between the studies and the pilot was the use of $AlCl_3$-salt as the aluminum source.

The use of $AlCl_3$-salt means a high Cl^- input (three times the amount of Al^{3+}). A high Cl^- concentration can be harmful for the environment (Verbruggen et al., 2008), but also increase the ionic strength of the groundwater, which increases the solubility of existing minerals (Öhman et al., 2006) and could

remobilize adsorbed contaminants (Wallace et al., 2012). Furthermore, production of aluminum chloride requires a large amount of energy (Choate and Green, 2003). There is therefore need for a new, cheaper, more environmentally friendly and natural available aluminum source.

The mineral gibbsite ($Al(OH)_3$) seems to meet these requirements as it is the main mineral of bauxite and the world's main source of aluminum. This leads to the idea that natural sources or even mine tailings could be used.

1.1. Research goal

The goal of this research is to investigate if gibbsite can be used as aluminum source to complex and precipitate with organic matter in the interest of soil permeability reduction. The research questions resulting from this goal are:

- Is it possible to dissolve gibbsite?
  - under which conditions?
  - what is the efficiency?
- Is it possible to form Al-DOM complexes under these conditions?
  - what is the efficiency?

1.2. Outline thesis

Chapter 2 starts with a graphical representation of all species and their mutual processes that are involved in this thesis. Followed by background information and a literature review of these species and processes. In Chapter 3 a description of materials that were used and the conducted experiments is given. The results from these experiments are given and discussed in Chapter 4. Leading to Chapter 5 in which the conclusions and outlook of this research are given.

2

Background: A literature study

This research aims to investigate the suitability of gibbsite as aluminum source to form complexes and precipitate with DOM in order to reduce soil permeability. Figure 2.1 gives a graphical representation of the species and processes relevant to this research. This chapter gives an overview and discussion of these species and processes and ends with hypothesis following from these discussions.

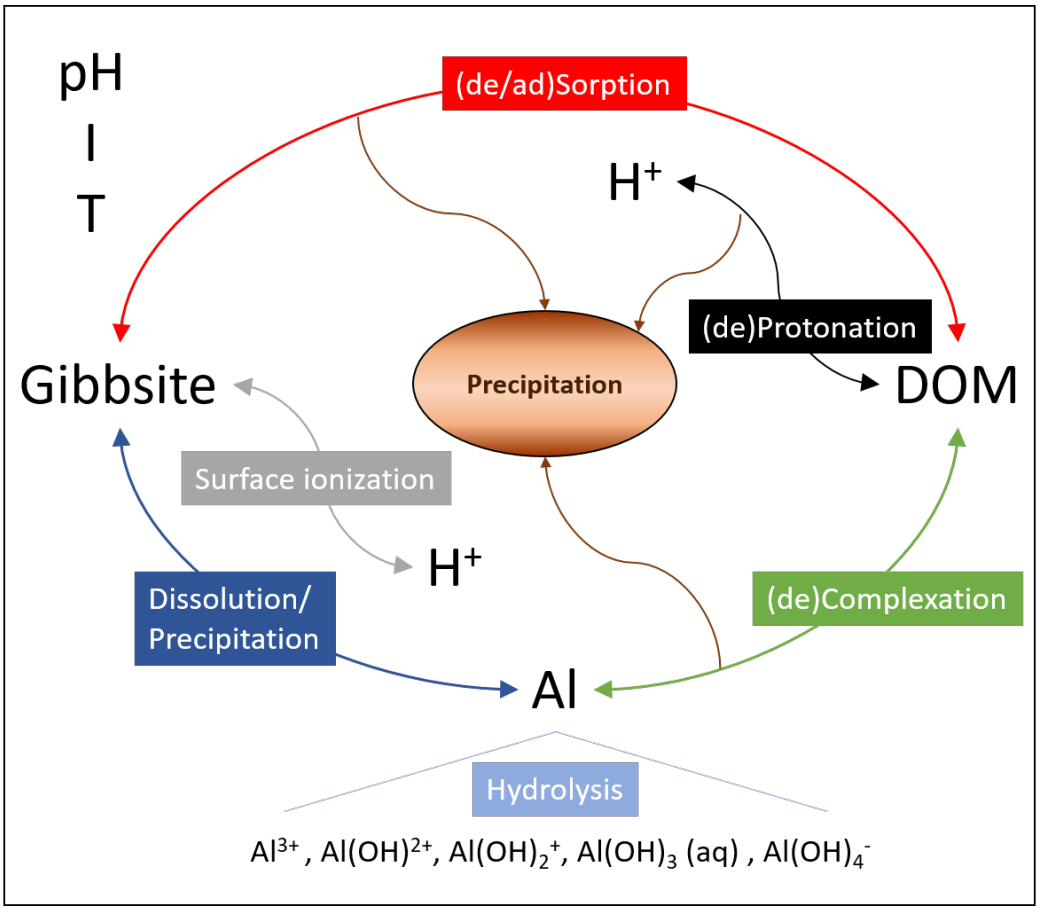

Figure 2.1: Graphical representation of the processes between the species: Gibbsite, free aluminum (Al) and Dissolved Organic Matter (DOM). Gibbsite can dissolve to free Al, which consists of different hydrolysis products. Free Al can complex with DOM and subsequently precipitate. Furthermore DOM can precipitate via protonation or adsorption to gibbsite, which can also adsorb H^+. All processes depend on the existence and amount of the species but also on the pH, Ionic strength (I) and Temperature (T) of the solution.

2.1. Particles in aqueous solution

Particles in aqueous solution are very likely to obtain a surface charge. This can have various reasons for example: the dissolution of constituent ions, isomorphous substitution and specific adsorption of ions (Gregory, 2005). But most commonly and the case for the species in this study, the surface has chemical groups that can ionize. The ionization mechanism of gibbsite and DOM will be discussed in respectively section 2.2.4 and section 2.3.2.

If a surface is charged there must be a corresponding excess of counter ions in solution to maintain electrical neutrality. The combined system is called an electrical double layer. With the surface charge being the first layer and the loosely associated counter ions surrounding the surface charge being the second layer (Gregory, 2005).

The electrical double layer is important for the adsorption to gibbsite (section 2.2.4) and in the flocculation of DOM (section 2.3.3). As approaching ions (i.e. H^+) and particles (i.e. DOM) are affected by it.

2.2. Gibbsite

This section starts with structural characteristics of gibbsite. Thereafter its solubility is discussed followed by the hydrolysis of aluminum. Lastly the adsorption of H^+ is discussed.

2.2.1. Characteristics

Gibbsite is the most common aluminum trihydroxide ($Al(OH)_3\,(s)$), occurring in (tropical) soils and as the major mineral in bauxite rocks (Hsu, 1977). Gibbsite exhibits polymorphism[1] (Hemingway and Sposito, 1996) and is composed of layers of two planes of close-packed OH^- ions with Al^{3+} in between (see figure 2.2) (Dixon and Weed, 1977). Single coordinated unsaturated hydroxide groups can ionize (in the figure depicted as H_2O).

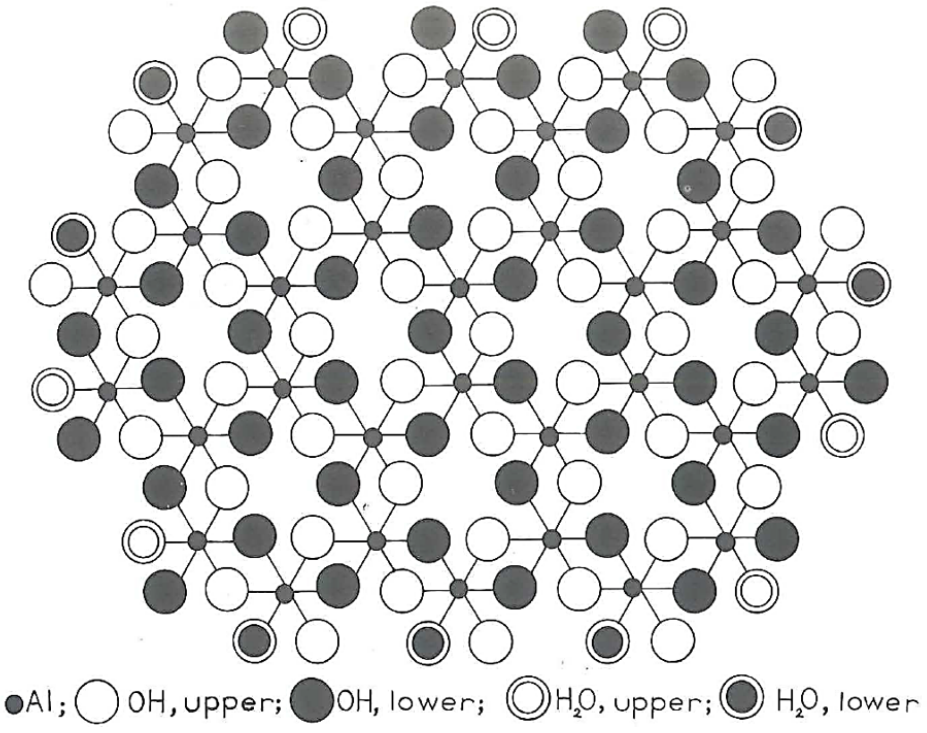

Figure 2.2: Schematic representation of one layer of gibbsite. Copied from Dixon and Weed (1977).

[1] crystal is made up of two or more identical compounds

The formation of gibbsite in nature happens through the precipitation of amorphous gibbsite and extended ageing (Karamalidis and Dzombak, 2010). With ageing the amorphous aluminum hydroxide crystallizes to crystalline gibbsite. The slow crystallization of gibbsite yields a high crystallinity making crystallized gibbsite a very stable mineral (Dixon and Weed, 1977).

Besides being abundant in nature gibbsite can also be synthesized. For example in the Bayern process[2] (Wefers and Misra, 1987). The difference between natural occurring gibbsite and synthesized gibbsite is that synthesized gibbsite has a higher crystallinity as naturally occurring gibbsite often contains impurities (Karamalidis and Dzombak, 2010). Furthermore the inter-planer distances in natural gibbsite are bigger (Yang et al., 2015). As a result from these differences, natural gibbsite is relatively more soluble than synthetic gibbsite (May et al., 1979; Wesolowski, 1992; Wefers and Misra, 1987; Yang et al., 2015).

2.2.2. Solubility

The dissolution of gibbsite can be described as:

$$\mathrm{Al(OH)_3(s) \longleftrightarrow Al^{3+} + 3\,OH^-}$$

The solubility constants reported for gibbsite are mainly on synthesized gibbsite and vary considerably, mostly because of difference in crystallinity (Lydersen, 1990). Reported solubility constants will therefore be divided into amorphous and crystallized solubility constants.

For amorphous gibbsite Duan and Gregory (2003) reported $\mathrm{LogK_{s,am}} = 10.5$, which is in agreement with the value that Hayden and Rubin (1974) found, $\mathrm{LogK_{s,am}} = 10.4$.

For crystalline gibbsite two broadly used values are by Lindsay (1979) $\mathrm{logK_{s,cr}} = 8.04$ and Palmer and Wesolowski (1992) $\mathrm{logK_{s,cr}} = 7.70$. Weng (2002) fitted these values and concluded that the latter was in good agreement with his measurements. This is in consonance with the findings of Wesolowski and Palmer (1994), $\mathrm{logK_{s,cr}} = 7.74$. The results of (Wesolowski and Palmer, 1994) are shown in 2.3, it can be seen that at low pH most gibbsite dissolves. At pH = 3 approximately 0.01 mol/L exists as free Al (it must be noted that this is at equilibrium).

The chemical equilibrium model visual MINTEQ, that is used in this thesis, has the following solubility constants in its database $\mathrm{logK_{s,am}} = 10.8$; $\mathrm{logK_{s,cr}} = 7.74$. These solubility constants fit well with the values from literature.

Dissolution rate

Research on the dissolution kinetics of gibbsite is mostly performed at high pH and temperatures, because these conditions are used in the Bayern process.

Grénman et al. (2010) researched the dissolution kinetics of gibbsite in concentrated sodium hydroxide solutions (2 M - 6 M) at 60-85 °C. They concluded that the dissolution rate is strongly positively dependent on increasing temperature, stirring rate and hydroxide concentration.

Bloom (1983) researched at acidic conditions (pH = 1.5 - 3) and 25 °C and stated that dissolution was not diffusion controlled but controlled by reactions at the solid-solution interface. This means that at low pH the gibbsite dissolution is independent of stirring rate. The findings of Ganor et al. (1999) supported this statement. Nagy and Lasaga (1992) did research at acidic conditions (pH=3) and 80 °C. They proposed a sigmoidal function for the dissolution rate depending on the deviation of the gibbs free energy of the reaction from the equilibrium value. From their research a constant dissolution rate far from equilibrium and very slow linearly decreasing dissolution rates near equilibrium are expected. Frink and Peech (1962), Wada and Kakuto (1999) and Su and Harsh (1994) reported on the slow kinetics of gibbsite dissolution, equilibrium was established after months.

[2] process of refining bauxite to produce alumina

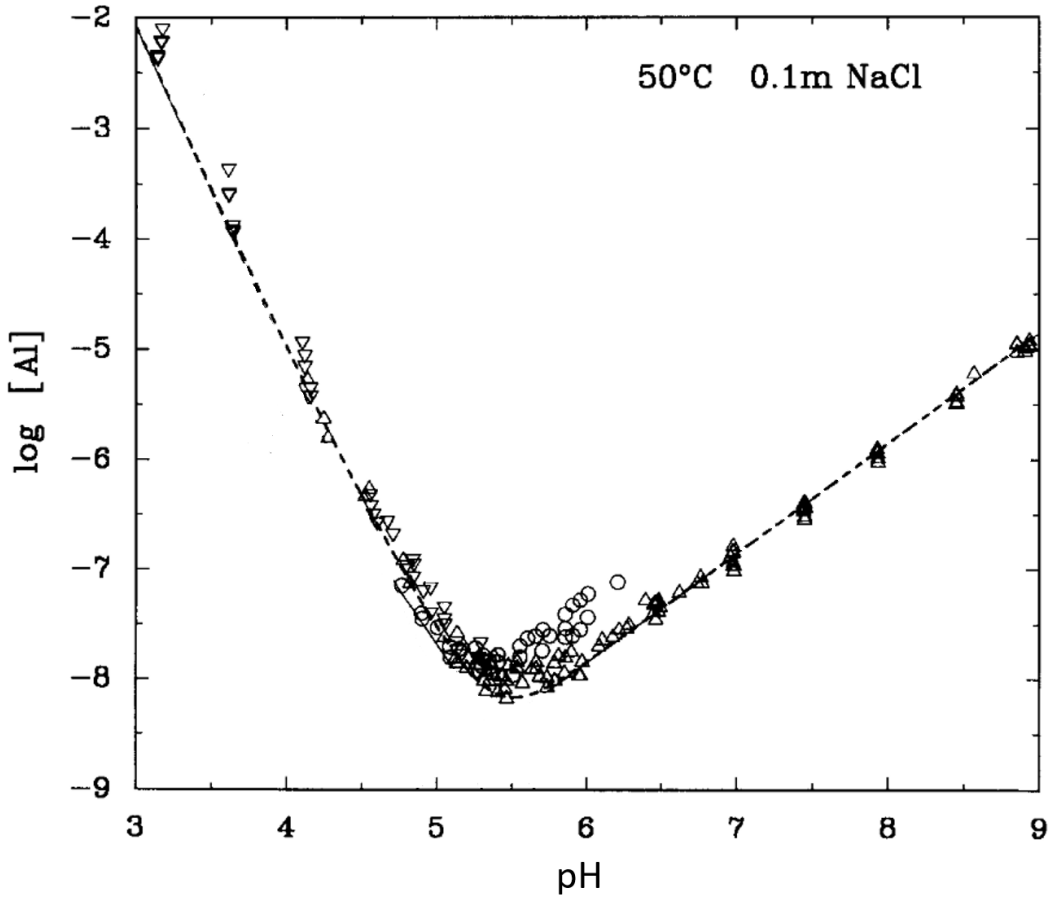

Figure 2.3: Concentration of Al in equilibrium with crystaline gibbsite in relation to pH. Modified after Wesolowski and Palmer (1994).

2.2.3. Hydrolysis

Al^{3+} is known to have a primary hydration shell consisting of six water molecules in octahedral coordination (Richens, 1997). The water molecules in this primary hydration shell are polarized. Depending on the pH this can lead to the loss of protons. This means that water molecules in the hydration shell can be progressively replaced by hydroxyl ions (Duan and Gregory, 2003), giving the so-called monomeric Al species:

$$Al^{3+} \longrightarrow Al(OH)^{2+} \longrightarrow Al(OH)_2{}^{+} \longrightarrow Al(OH)_3 \longrightarrow Al(OH)_4{}^{-}$$

Many researchers report the existence of aluminum dimer, trimer and polymers (Duan and Gregory, 2003; Ekberg and Brown, 2016; Xiao et al., 2008). However, research has shown that they do not occur in significant proportions (Martin, 1991; Van Benschoten and Edzwald, 1990; Xiao et al., 2008), especially not at low ionic strength (Ekberg and Brown, 2016). The hydrolysis of aluminum can therefore be described by the monomeric Al species. The successive deprotonations can then be given by the following equations and hydrolysis constants[3] (Wesolowski and Palmer, 1994):

$$Al^{3+} + H_2O \longleftrightarrow Al(OH)^{2+} + H^{+} \qquad \log K_1 = -4.95$$

$$Al(OH)^{2+} + H_2O \longleftrightarrow Al(OH)_2{}^{+} + H^{+} \qquad \log K_2 = -5.60$$

$$Al(OH)_2{}^{+} + H_2O \longleftrightarrow Al(OH)_3(aq) + H^{+} \qquad \log K_3 = -6.70$$

$$Al(OH)_3(aq) + H_2O \longleftrightarrow Al(OH)_4{}^{-} + H^{+} \qquad \log K_4 = -5.60$$

[3]Constants are at zero ionic strength and 25°C

Using these hydrolysis constants and $\mathrm{LogK_{s,am}} = 10.5$ Duan and Gregory (2003) plotted the concentrations of the various species in equilibrium with amorphous hydroxide as a function of pH (see figure 2.4). It can be seen that under acidic conditions $\mathrm{Al^{3+}}$ predominates whereas under neutral and base conditions $\mathrm{Al(OH)_4{}^-}$ predominates. Comparing the concentrations of the Al species in equlibrium with amorphous hydroxides (figure 2.4 right) with the concentrations at equlibrium with crystalline hydroxide (figure 2.3) it is visible that crystalline gibbsite dissolves much less.

The hydrolysis (and dissolution) constants depend highly on: temperature (Lydersen, 1990; Wesolowski and Palmer, 1994), due to the temperature dependency of the ion product of water (Van Benschoten and Edzwald, 1990), and ionic strength (Wesolowski and Palmer, 1994; Öhman et al., 2006).

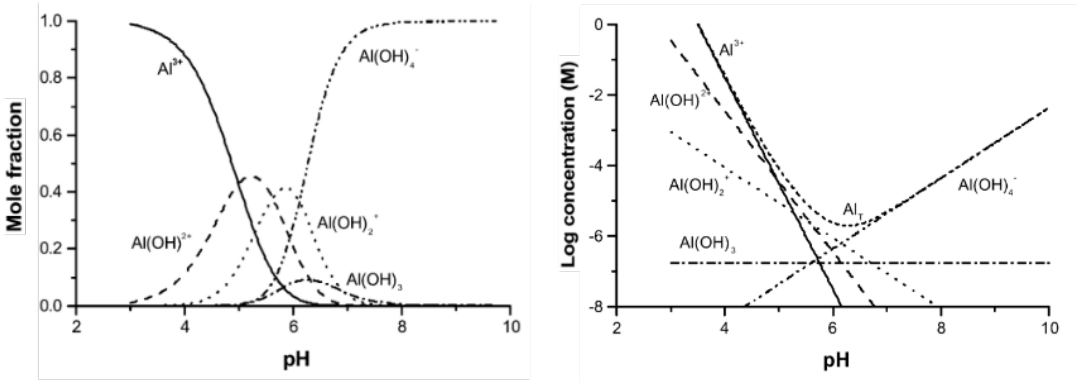

Figure 2.4: Left: Proportions of Al hydrolysis species in equilibrium with amorphous gibbsite. Copied from Duan and Gregory (2003). Right: Concentrations of Al hydrolysis species in equilibrium with amorphous gibbsite. Copied from Duan and Gregory (2003).

2.2.4. Adsorption

The surface of gibbsite can ionize, the surface ionization reactions can be expressed by a so called 2-pK formalism (Karamalidis and Dzombak, 2010). Which means that the surface acid-base behaviour is described by the following two reactions:

$$\equiv \mathrm{AlOH_2{}^+} \longleftrightarrow \equiv \mathrm{AlOH^0} + \mathrm{H^+} \qquad \mathrm{K_{a1}^{app}}$$

$$\equiv \mathrm{AlOH^0} \longleftrightarrow \equiv \mathrm{AlO^-} + \mathrm{H^+} \qquad \mathrm{K_{a2}^{app}}$$

with:

$$\mathrm{K_{a1}^{app}} = \frac{(\equiv \mathrm{AlOH^0})\{\mathrm{H^+}\}}{(\equiv \mathrm{AlOH_2{}^+})}$$

$$\mathrm{K_{a2}^{app}} = \frac{(\equiv \mathrm{AlO^-})\{\mathrm{H^+}\}}{(\equiv \mathrm{AlOH^0})}$$

When using a diffuse layer model (DLM) to describe the adsorption of $\mathrm{H^+}$ to gibbsite the $\mathrm{K_{a1}}^{\mathrm{app}}$ and $\mathrm{K_{a2}}^{\mathrm{app}}$ are apparent equilibrium constants because they include electrostatic contributions. This means that they are dependent on the extent of surface ionization. To separate the chemical and electrostatic contributions (theoretically) a variable electrostatic interaction term needs to be added, the so-called Boltzmann factor. This leads an intrinsic equilibrium constant which does not depend on surface charge:

$$\mathrm{K_{a1}^{int}} = \frac{(\equiv \mathrm{AlOH^0})\{\mathrm{H^+}\}}{(\equiv \mathrm{AlOH_2{}^+})} \mathrm{e}^{\frac{\Delta \mathrm{ZF}\Psi}{\mathrm{RT}}}$$

$$\mathrm{K_{a2}^{int}} = \frac{(\equiv \mathrm{AlO^0})\{\mathrm{H^+}\}}{(\equiv \mathrm{AlOH^0})} \mathrm{e}^{\frac{\Delta \mathrm{ZF}\Psi}{\mathrm{RT}}}$$

where ΔZ is the change of equivalent charge taking place in the reaction (in this case with H^+, ΔZ = -1), F is the Faraday constant (96.485 C/mol), Ψ is the surface potential (V), R is the common gas constant (8.314 J / (K mol)) and T is the temperature (K).

The pH at which the surface has zero net proton charge is called the point of zero net proton charge (PZNPC). If H^+ is the only adsorbing ion the PZNPC is equal to the point of zero charge (PZC), this is known as the pristine point of zero charge (PPZC). The PPZC gives the pH at which the number of negatively and positively charged sites is equal and the surface is uncharged. This point is halfway between the two acidity constants and can be calculated with:

$$\mathrm{PPZC} = \frac{1}{2}\left(\mathrm{pK}_{\mathrm{a1}}^{\mathrm{int}} + \mathrm{pK}_{\mathrm{a2}}^{\mathrm{int}}\right)$$

Karamalidis and Dzombak (2010) did an extensive study using data from 13 titration's from various studies on the intrinsic surface acidity constants. The weighted averages found were $\log \mathrm{K}_{\mathrm{a1}}^{\mathrm{int}} = -7.17$ and $\log \mathrm{K}_{\mathrm{a2}}^{\mathrm{int}} = -11.18$. From this follows PPZC = 9.17, which is close to values found in literature, which means that below a pH of 9.17 H^+ is adsorbed to gibbsite.

The full DLM Dzombak created especially for gibbsite is integrated in visual MINTEQ and used in this thesis. A more detailed description of the DLM can be found in (Dzombak and Morel, 1990; Karamalidis and Dzombak, 2010)

2.3. Organic Matter (OM)

This section starts with the classification of OM. Secondly the solubility of OM and the importance of its functional groups is explained. Thereafter the stability of OM is discussed. Lastly potassium humate will be described.

2.3.1. Characteristics

Natural organic matter in soils consist of litter, other plant residues, soil biomass and humus (Stevenson, 1994). From these, humus is the stable end product of the degradation of the other substances and predominates in most soils (Tipping, 2002). Humus can be divided in humic substances and non humic-substances. Humic substances are a series of unidentifiable organic compounds of relatively high molecular weight. Non-humic substances are identifiable and can be placed in categories as sugars, amino acids etc. (van Zomeren, 2008). The majority of the organic carbon in soils, natural waters and their sediments is present as humic matter (Tipping, 2002).

Humic substances are classically fractionated in three main fractions based on their solubility (Tipping, 2002; van Zomeren, 2008; Stevenson, 1994):

1. *Humin*, insoluble in acid and base
2. *Humic acids (HA)*, soluble in base and insoluble in acid
3. *Fulvic acids (FA)*, soluble in both acid and base

The division is given as a scheme in figure 2.5. Generally HA is defined as completely insoluble below pH = 2. Humin, HA and FA are old-fashioned terms and are of minor use for a precise description of many soil processes on a molecular level. They are however used in this thesis because they have been used in many (recent) studies, because of a lack of a proper redefinition of humic substances.

Another often used division is based on molecular weights. Distinguishing high molecular weight acids (HMW) and low molecular weight (LMW) acids. HA an FA are considered to be high molecular weight acids with molecular weights of >3000 g/mol for HA, 1000– 3000 g/mol for FA. LMW acids are defined by <1000 g/mol (Lundström et al., 2000a).

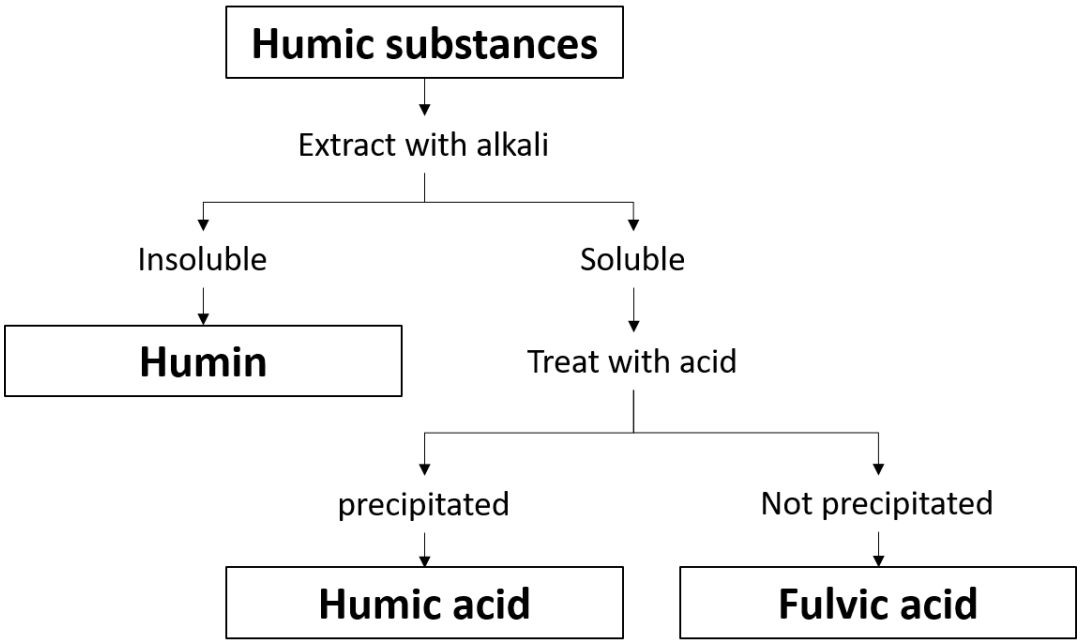

Figure 2.5: Classification of humic substances. Modified after van Zomeren (2008).

2.3.2. Solubility

A distinction between DOM and OM is made by filtration, with a 0.45 µm filter (Weng, 2002; Zsolnay, 2003).

DOM obtains its solubility from two important functional groups that can ionize: carboxylic and phenolic groups (Motta et al., 2016; van Zomeren, 2008). Ionized groups interact with water molecules, this interaction makes the DOM molecule more hydrophilic. The ionization of phenol and carboxylic acid are given by the following equations and constants: (de Ruiter, 2005a):

Carboxylic:

$$\mathrm{RCOOH} \longleftrightarrow \mathrm{RCOO^-} + \mathrm{H^+} \qquad \mathrm{logK} = -4$$

Phenolic:

$$\mathrm{ROH} \longleftrightarrow \mathrm{RO^-} + \mathrm{H^+} \qquad \mathrm{logK} = -10$$

It can be concluded that carboxylic groups are relatively strong acids that ionize at low pH whilst phenolic groups are relatively weak acids that dissociate at high pH. It is important to note that the acidity of both functional groups varies widely, depending on the overall structure of the acids (de Ruiter, 2005b; Reusch, 2014; Stevenson, 1994).

A phenolic group is roughly a million times more acidic than an equivalent alcohol group (logK = -16) because of the electron withdrawing capacity of the benzoic ring to which the alcohol group of a phenolic group is attached (Reusch, 2014). The same way, the acidity of phenolic and carboxylic groups can be (further) enhanced by electron-withdrawing groups (e.g. benzoic or $\mathrm{Cl^-}$) or decreased by electron-donating groups (e.g. methyl) (de Ruiter, 2005b). This effect is shown by the pK (pK = -logK) distribution curve Manunza et al. (1992) created, shown in figure 2.6. As a result a titration curve of humic (and fulvic) acids has a ”smeared out” S-shape appearance (see figure 2.7).
Besides the apparent pH dependency of the solubility of OM, it also depends on ionic strength. The solubility of OM decreases with increasing ionic strength (Tipton et al., 1992).

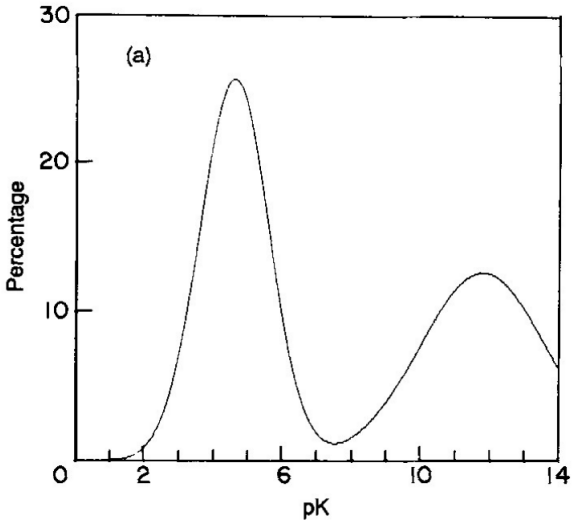

Figure 2.6: pK distribution function of a humic acid, calculated with a model based on well fitted humic acid titration tests. Copied from Manunza et al. (1992).

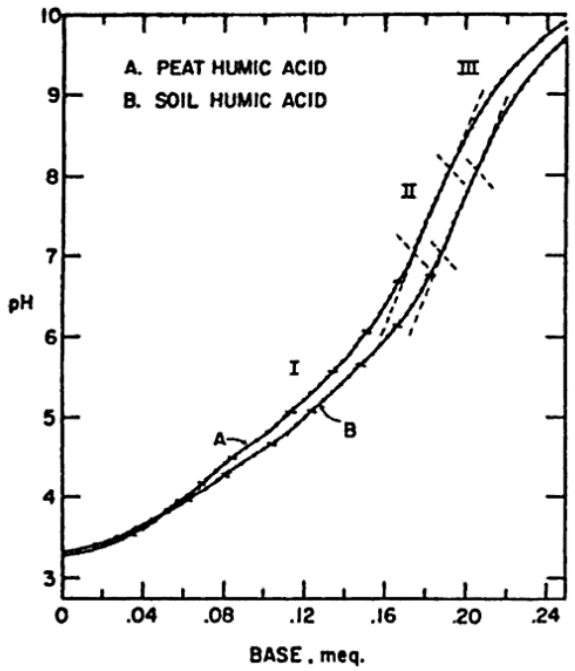

Figure 2.7: Titration curve of two humic acids. Three zones are indentified, seperated by the dotted lines. Zone I is the region where carboxylic groups ionize, zone III is the region where phenolic groups ionize and zone II is the region where ionization of both groups overlap. Copied from Stevenson (1994).

2.3.3. Stability

Colloid interactions happen on a short range (usually smaller than the particle size). These interactions therefore happen when particles are nearly in contact. There are three significant ways particles come into contact (Gregory, 2005):

- *Brownian diffusion*, collisions caused by random movements all particles in aqueous solution undergo, as a results of thermal energy.
- *Fluid motion*, collisions caused by any form of shear by for example stirring or flow.
- *Differential sedimentation*, collisions caused by a difference in settlement rate.

If particles come into contact there are two important colloid interactions:

- *van der Waals forces*, the attraction between dipoles.
- *Electrical double layers*, as discussed in section 2.1, charged particles carry an electrical double layer. When two charged particles come close together their double layers interact. Particles with similar charge repulse each other.

Combining the two interactions gives the potential energy diagram (figure 2.8), with the important feature of an energy barrier. Particles approaching each other have to have a combined energy (from the collisions mechanisms) exceeding this barrier to come into contact.

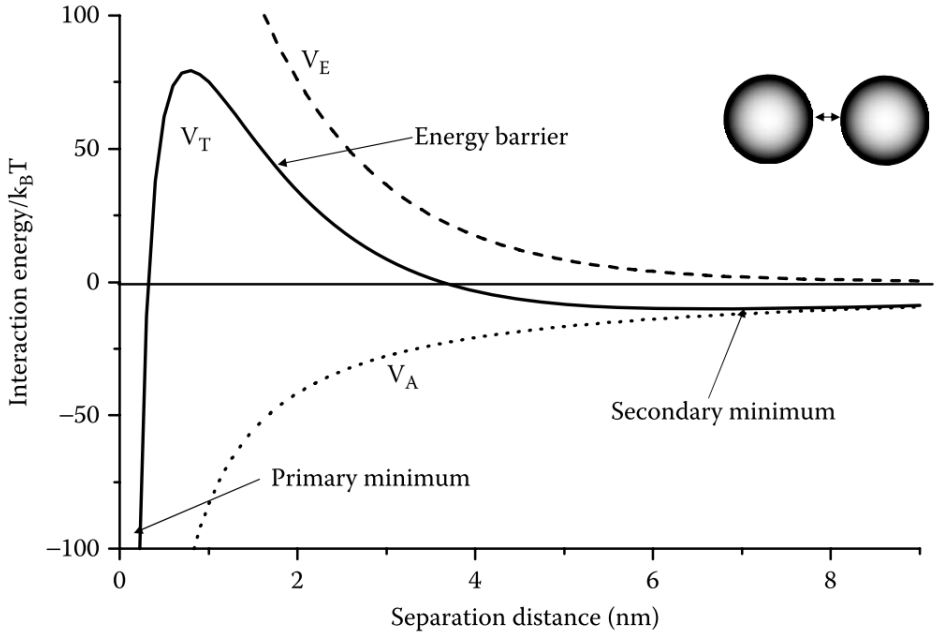

Figure 2.8: Potential energy diagram, with electrical (VE), van der Waals (VA) and total interaction energy (VT). Modified after (Gregory, 2005).

This means that when pH decreases, protonation of the functional groups means less surface charge and therefore a smaller energy barrier, creating the possibility for DOM-DOM aggregation.

The ionic strength of a solution has a strong twofold influence on the stability of DOM. Firstly, at higher ionic strength the diffuse layer of the electrical double layer becomes smaller, thereby lowering the energy barrier. Secondly DOM can be seen as polymers. Ionized functional groups repulse each other stretching out the DOM. Repulsion between the functional groups is oppressed at increasing ionic strength in the same way it reduces the width of the diffuse layer.

When lowering the pH (by adding acid and thereby increasing the ionic strength), the stability and subsequently the solubility of DOM is affected in the following ways (mechanisms are schematically given in figure 2.9):

1. Protonation of the functional groups makes the particle more hydrophobic subsequently due to charge neutralization the polymeric DOM rearranges to a more random coil figuration, thereby increasing its density.
2. Protonation of the functional groups lowers the energy barrier for DOM particles to interact and aggregate, thereby becoming more hydrophobic.
3. An increase in ionic strength compresses the polymeric DOM to rearrange to a more random coil figuration, thereby increasing its density.
4. An increase in ionic strength compresses the diffuse layer of particles and subsequently lowers the energy barrier for DOM particles to interact and aggregate, thereby becoming more hydrophobic.

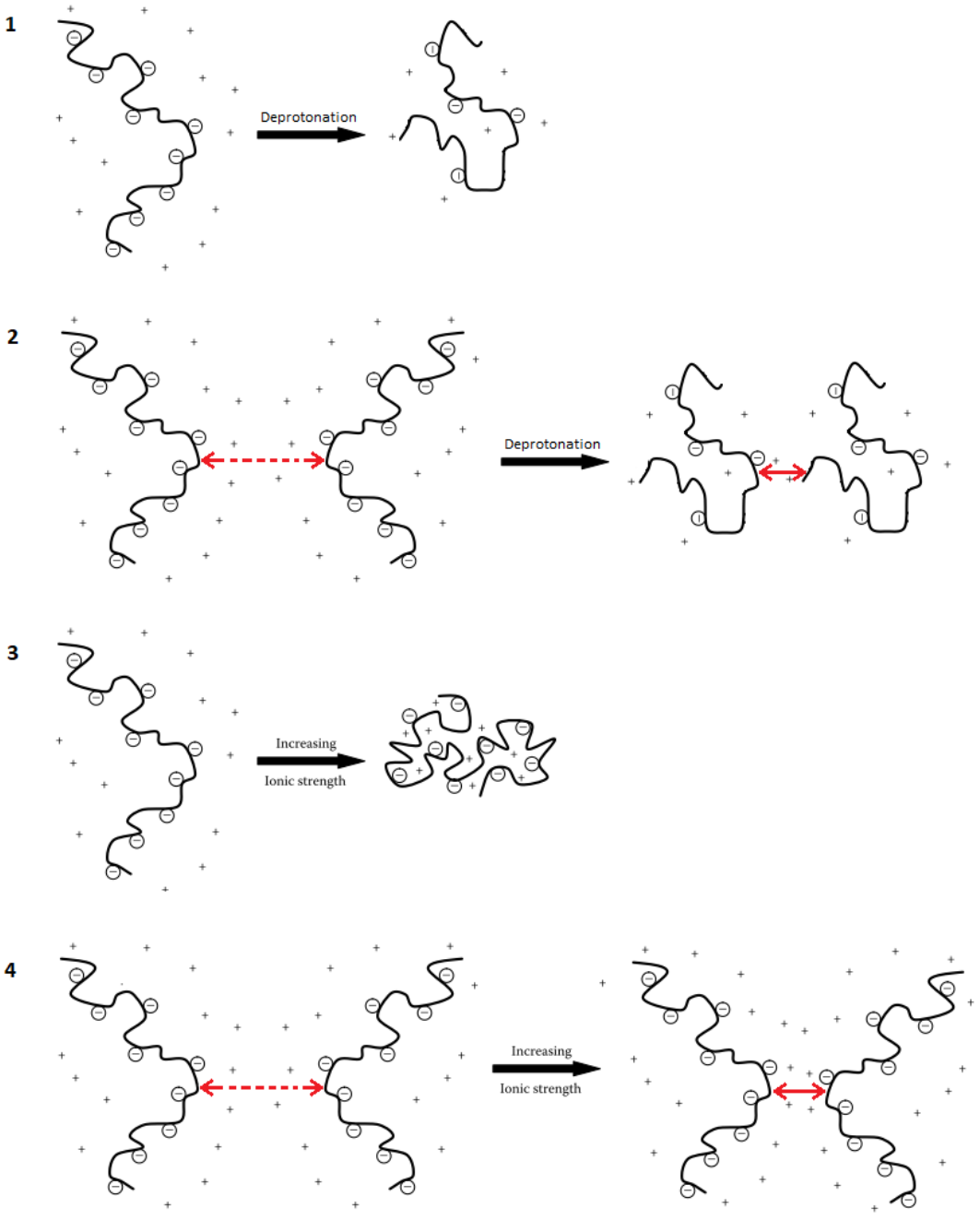

Figure 2.9: Mechanisms lowering the stability of DOM when lowering the pH.

2.3.4. Potassium humate

In this theis a potassium humate is used. Potassium humate is the potassium salt of humic acid, derived from lignite brown coal (Kumar et al., 2013). A fraction of the protons from its functional groups have been displaced by potassium (Levinsky, 2008). Stevenson (1994) proposed a general structure of potassium humate given in figure 2.10. When a potassium humate is brought in aqueous solution, the non-reactive potassium dissociates and some functional groups protonate again (reaction is given below). As a result a potassium humate solution has a high pH.

$$\mathrm{RCOOK + H_2O \longleftrightarrow RCOOH + K^+ + \textbf{OH-}}$$

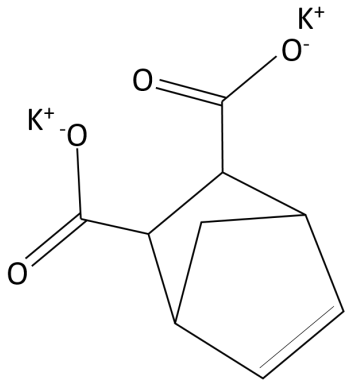

Figure 2.10: General structural formula of potassium humate. Reproduced from Kumar et al. (2013).

2.4. DOM and gibbsite or free aluminum

This section describes two phenomena. Firstly the adsorption of DOM onto gibbsite and secondly the complexation between DOM and free aluminum.

2.4.1. Adsorption

Adsorption of DOM onto gibbsite can occur via the formation of inner-sphere or outer-sphere complexes. Inner-sphere complexes are formed by the replacement of one (or more) hydroxide ions (or water molecules) from gibbsite by DOM. This way a direct bond exist between the metal ion, at the gibbsite surface, and one or several functional groups of the DOM. Depending on the composition and structure of DOM many inner-sphere complex coordinations are possible (Evanko and Dzombak, 1998; Guan et al., 2006c). In outer-sphere complexes no hydroxide ions are replaced. The complexes are formed because of attraction due to opposite surface charge and hydrogen bonding (Nordin et al., 1997). The formation reactions are described by:

Outer-sphere:

$$\mathrm{\equiv SOH_2{}^+ + DOM^- \longleftrightarrow \equiv SOH_2{}^+DOM^-}$$

Inner-sphere:

$$\mathrm{\equiv SOH + DOM^- \longleftrightarrow \equiv SDOM + OH^-}$$

Carboxylic and phenolic groups are considered to dominate the adsorption behaviour of DOM. The maximum adsorption through carboxylic groups occurs at pH ± 4, whereas the maximum adsorption through phenolic groups appears at pH ± 9 (Guan et al., 2006b). At these maxima there is an optimal balance between the degree of the functional groups deprotonation and surface ionization of gibbsite (Schneckenburger et al., 2018). The amount of deprotonated groups increase with rising pH, while the number of positive charges on the gibbsite surface decrease with increasing pH. Because the carboxylic groups protonate at much lower pH the adsorbed amount of DOM reach a maximum at pH 4 – 5.5 mainly due to the adsorption of carboxylic groups forming outer-sphere complexes (Schneckenburger et al., 2018).

From this it can be concluded that carboxylic groups are of primary importance in the adsorption of DOM onto gibbsite. But many researchers underlined the importance of phenolic groups (Davis and Leckie, 1978; Guan et al., 2006c). For example the presence of phenolic groups close to a carboxylic group can increase the electron density within the carboxylic group, thereby increasing its capacity to form gibbsite-carboxylic inner-sphere complexes (Guan et al., 2006c).

The adsorption mechanism of DOM is influenced by many aspects, as the: carboxylic content, phenolic content, positions of these groups, aromaticity and temperature (Evanko and Dzombak, 1998; Guan et al., 2006a,b; Korshin et al., 1997; Rosenqvist et al., 2003). But adsorption can be mainly attributed to carboxylic outer-sphere complexation with a maximum around pH = 4 (Nordin et al., 1998; Schneckenburger et al., 2018).

In this thesis adsorption of DOM onto gibbsite is considered to be only due to outer-sphere complexes, therefore not affecting the pH.

2.4.2. Complexation

Al and DOM can form complexes, the positively charged Al ion (lewis acid) reacts with the negatively charged functional group(s) of DOM (lewis base) forming a covalent bond. A part of the negative charge of DOM is thereby compensated, potentially changing its solubility (Weng, 2002).

Similarly as for DOM adsorption onto gibbsite, complexation between dissolved Al and DOM can be due to inner- and outer-sphere complexes. The formation of outer-sphere complexes is relatively fast in comparison to inner-sphere complexation, but inner-sphere bonds are stronger (Sposito, 2008).

The formation of soluble $\mathrm{Al{-}DOM}$ complexes happens fast (Vis, 2015). Furthermore it is pH dependent (Hagvall et al., 2015; Weng, 2002), as at higher pH more functional groups are deprotonated (section 2.2.2), whereas at lower pH more Al^{3+} is present (section 2.2.3).

Jansen et al. (2001, 2003) and Nierop et al. (2002) investigated the pH dependency of $\mathrm{Al{-}DOM}$ complexation and precipitation in combination with Al/C ratio. The results of Jansen et al. (2003), shown in figure 2.11, show the pH and Al/C ratio (molar) dependency of $\mathrm{Al{-}DOM}$ complexation and precipitation. Initially, at low Al/C, the soluble $\mathrm{Al{-}DOM}$ complexes were dominant at all three pH's. With increasing Al/C ratio different behaviour per pH level was observed. At all pH levels the fraction of soluble $\mathrm{Al{-}DOM}$ complexes decreased but a profound difference in the precipitated fraction was found. At pH = 3.5 it stayed the lowest fraction until Al/C > 0.1 whereas at pH = 4.5 a sharp increase in $\mathrm{Al{-}DOM}$ precipitates was observed at Al/C > 0.03. These results are supported by the results of Nierop et al. (2002). Additionally they added the fraction of precipitated C at different pH levels with increasing Al/C ratio (molar) (figure 2.12), thereby emphasizing the sharp increase of precipitation at Al/C = 0.03.

The complexation of Al and DOM depends on pH because of an optimum between DOM deprotonation and Al hydrolysis. The formation of insoluble complexes therefore highly depends on the DOM type but seem to have an optimum around pH = 4.5. As Al is still available as Al^{3+} but more functional groups are deprotonated then at lower pH. Moreover the formation of insoluble complexes requires a certain Al/C ratio, which seems to be at least 0.03.

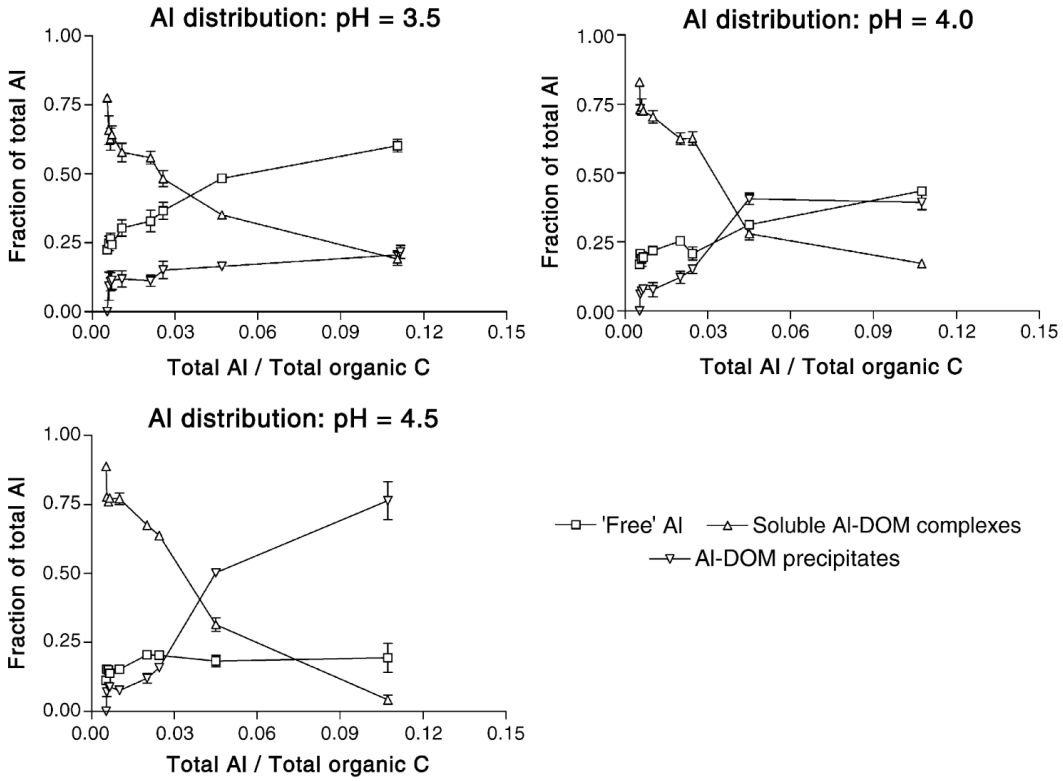

Figure 2.11: Fractional distribution of total Al over free Al, soluble Al−DOM complexes and Al−DOM precipitates in relation to molar Al/C ratio at pH = 3.5 ; 4 ; 4.5. Copied from Jansen et al. (2003).

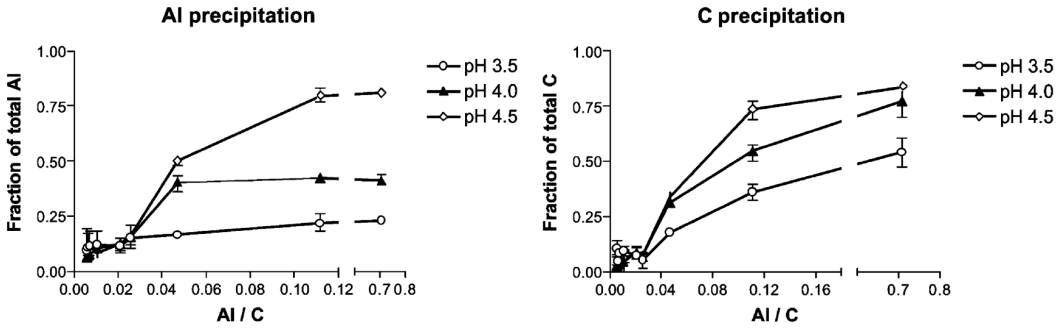

Figure 2.12: Fraction of precipitated Al (in Al−DOM complexes) in relation to molar Al/C ratio (left), and fraction of precipitated C (in Al−DOM complexes) in relation to molar Al/C ratio (right). Copied from Nierop et al. (2002).

2.5. Hypotheses for experiments

From all the processes depicted in figure 2.1, the goal is to achieve precipitation via complexation. For this process to happen gibbsite needs to dissolve to Al and DOM needs to stay soluble. From the background laid out in the previous sections a few hypothesis are formulated regarding these processes and the conditions for them to take place. Because all processes are pH depended the hypothesis are divided based on pH.

Low pH
At low pH gibbsite dissolution to Al^{3+} is expected. At equilibrium pH = 3 0.01 mol/L Al^{3+} is predicted but because the dissolution kinetics are very slow lower values are expected.
At pH $\leq$ 2 potassium humate is expected to be completely insoluble.

Transitional pH range
Because gibbsite dissolution happens most profound at low pH and potassium humate is insoluble at low pH, it is expected that at a narrow pH range conditions favour complexation. In this transitional zone it is expected to still have gibbsite dissolution and soluble OM. Complexation of Al and DOM might increase the dissolution rate.

Neutral pH
At neutral pH gibbsite dissolution is at its minimum and can be regarded as zero. OM is expected to be soluble. No significant adsorption or complexation is expected.

High pH
At high pH gibbsite dissolution to $Al(OH)_4^-$ and soluble OM is expected. No complexation between OM and $Al(OH)_4^-$ is foreseen. It must be noted that in this thesis very basic conditions are not researched.

3

Materials and methods

The goal of this research is to investigate the suitability of gibbsite as aluminum source to complex and precipitate with organic matter. To achieve this goal some experiments were set up investigating the processes (described in the theory, section 2) of and between gibbsite and OM.

This chapter describes the conducted experiments but addresses the materials (section 3.1) and measurements (section 3.2) used in these experiments first. The experiments are divided into two series (sections 3.3 & 3.4). Each series consisted of multiple experiments and each experiment consisted of a certain amount of samples. The following coding is used to describe the samples from all the experiments:

$$Ex.ySz$$

with x = series number, y = experiment number and z = sample number

3.1. Chemicals

The chemicals that were used in the experiments are organic matter, Gibbsite and acids. In this section each chemical is shortly addressed.

3.1.1. Organic matter

The organic matter source that has currently been used in the SoSEAL project and in this thesis is HUMIN-P775 (CAS - 68514-28-3), from now on abbreviated to HUMIN. It is a black powdered potassium humate (see 2.3.4) produced by Humintech (see figure 3.1).

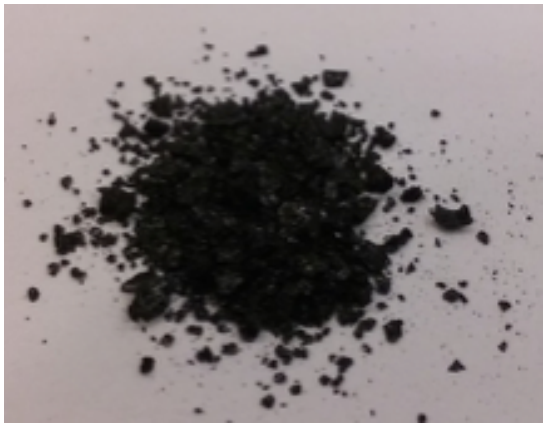

Figure 3.1: Photo of dry HUMIN-P775

The Al/C ratio (mol/mol) is an important parameter in the DOM and aluminum interaction (section 2.4.2). Therefore it is important to know the carbon content of HUMIN. At the Univerisy van Amsterdam (UvA) an elemental analysis (CHNS analysis) has been carried out on HUMIN, given in table 3.1. With these results, assuming that HUMIN is fully soluble in pure water, it can be calculated that a 3 g/L HUMIN solution contains approximately 0.1 mol C/L.

Table 3.1: Elemental analysis on HUMIN

Sample ID	Total N (wt%)	Total OC (wt%)	Total H (wt%)	Total S (wt%)
Humic_01	1.05	41.81	3.12	0.83
Humic_02	1.00	42.54	3.83	0.88
Average	1.03	42.18	3.48	0.85

3.1.2. Gibbsite

A white coloured well crystallized gibbsite powder (CAS 21645-51-2) produced by Sigma-Aldrich is used (see Figure 3.2). In aqueous solution it forms a colloidal suspension with 90% of the grains smaller than 150 μm. Hereafter it will be referred to as gibbsite, whereas the described dissolved species will be referred to as Al.

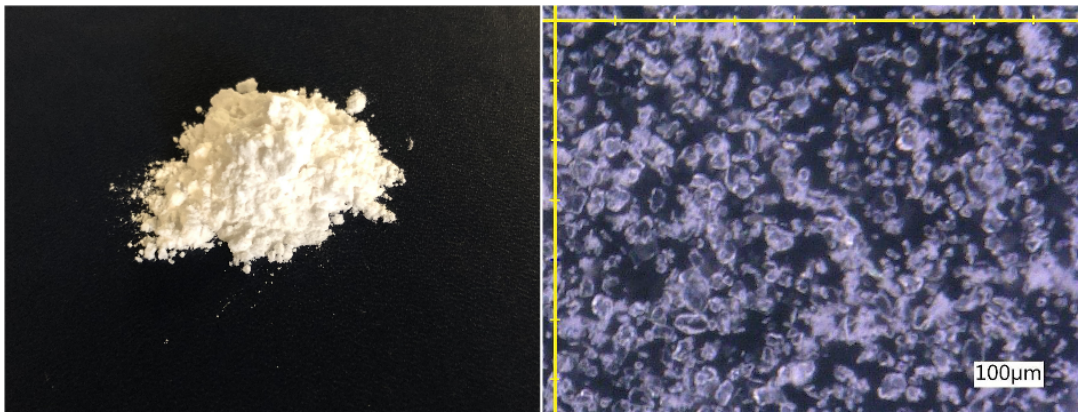

Figure 3.2: Left: Photo of dry gibbsite powder ; Right: Gibbsite suspension under microscope.

3.1.3. Acids

The acids used to control the pH in the experiments are 0.1 M and 1.6 M HCl. HCl was used because the counter ion, Cl^-, is assumed to be non-reactive.

3.2. Measurements

pH and EC measurements were performed using a Consort 3010 apparatus. Calibration of the pH and EC electrodes were performed on a daily basis using buffer solutions of EC: 0.01 M and 0.1 M KCl and pH: 4, 7 and 10.

DOM concentrations were measured using UV measurements at 254 nm as UV adsorbance at 254 nm is proportional to DOM concentration (Zhang, 2013; Deflandre and Gagné, 2001). For the UV measurements two types of cuvettes with different diameters were used, because not enough cuvettes of a single type were available. The calibration lines, created with known concentrations of DOM, for both cuvette types are given in figures 3.3 and 3.4. The UV measurements are unreliable when the absorbance is bigger than 2.5 (-), it was therefore chosen to accept UV measurements with absorbance within the range of 0.4 – 2 (-). The HUMIN concentrations used in the experiments were far higher than the DOM concentrations corresponding with UV absorbance within this range. Dilution of the samples was therefore needed, with dilution factors varying between 2 - 40. Dilution was accomplished by adding the appropriate amount of sample volume and demineralized water to a total of 2 mL. As

discussed in section 2.3.2 DOM is defined as the fraction of OM that is smaller than 0.45 μm. Due to the high HUMIN concentrations applied in the experiments (up to 3 g/l) filtration was impossible, because of clogging, and therefore disregarded. Sampling for the DOM measurements was performed by extracting the necessary volume from a undisturbed sample just below the sample's surface. It is therefore assumed that all measurements were in fact measurements of *Dissolved* OM.

Al concentrations were measured using a standard Hach Lange aluminum measurement kit and UV adsorbance at 620 nm. The kit measures free aluminum within the range of 0.02 – 0.5 mg/L Al (Hach, 2013). Dilution of the sample with pure water was therefore needed with dilution factors varying between 20 – 30. The variation coefficient[1] of the kit is 2.2 % (König, 2007).

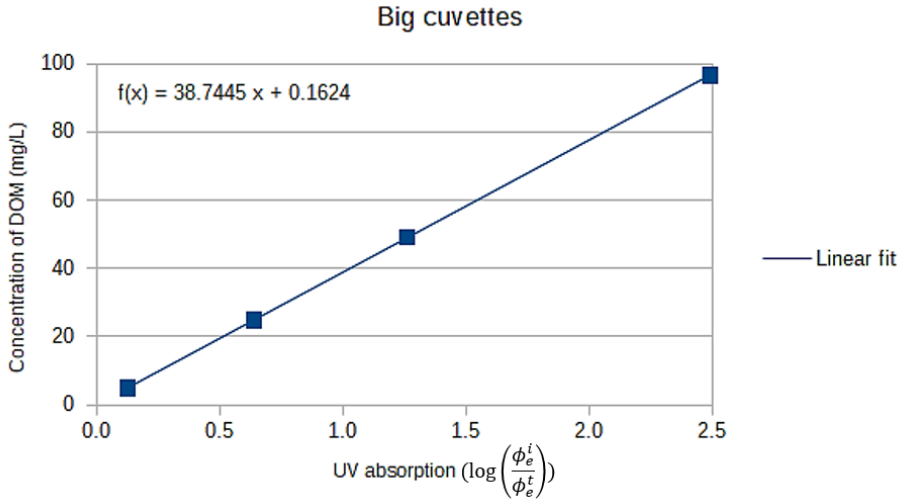

Figure 3.3: Relationship between the concentration of DOM and the absorbtion of UV light at 254 nm.

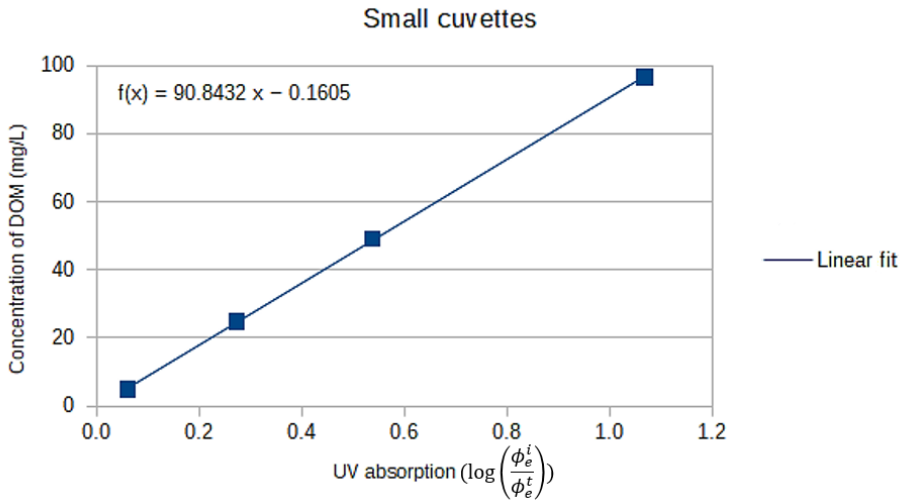

Figure 3.4: Relationship between the concentration of DOM and the absorbtion of UV light at 254 nm.

[1]The variation coefficient is the ratio of the standard deviation over the mean

3.3. Experiment series 1 (E1.ySz)

For the first series of experiments stock solutions/suspensions of HUMIN and gibbsite were prepared with a of concentration 3 g/L (0.1 mol C/L) and a amount of 7.8 g/L (0.1 Al-mol/L) respectively. Before preparing any sample the stock solutions were shaken vigorously.

3.3.1. Gibbsite at low pH; E1.1Sz

To gain insight in the adsorption and dissolution behaviour of gibbsite at a low pH range, 100 mL of pure gibbsite stock suspension was taken and distributed over five samples (all containing approximately 20 mL). The initial pH was just above 7 and the initial EC around 21 μS/cm. The pH of the samples was adjusted with 0.1 M HCl so that they ranged from 2.0 to 3.3.

Eighteen pH and EC measurements were performed during 41 days. In the beginning measurements were performed on a daily basis whereas in the end a maximum of one week in between measurements was used.

3.3.2. HUMIN at low pH; E1.2Sz

To describe the behaviour of HUMIN at a low pH range four samples with approximately 20 mL of pure HUMIN stock solution were created. The initial pH was around 9.5. The pH of the samples was adjusted with 0.1 M and 1.6 M HCl so that they ranged from 1.5 to 3.0.

Eight pH, EC and UV-DOM measurements were performed during 28 days.

3.3.3. HUMIN + gibbsite with differing pH; E1.3Sz

In this experiment the effect of pH on the behaviour of HUMIN plus gibbsite was investigated. A solution/suspension with a Al/C ratio of 0.1; $pH_{initial}$ = 9.67 and $EC_{initial}$ = 575 µS/cm was created by mixing 200 mL of pure HUMIN stock solution and 20 mL of pure stock gibbsite suspension and stirring it for 3 minutes. This solution/suspension was distributed over eight samples, with approximately 20 mL each. The pH of the samples was then adjusted with 0.1 M HCl so that they ranged from 2 to 9 with increments of ± 1.

Nine pH and EC measurements were performed during 41 days.

3.3.4. HUMIN + gibbsite with differing Al/C ratio; E1.4Sz

In this experiment the effect of the Al/C on the behaviour of HUMIN plus gibbsite was investigated. The pH of approximately 120 mL pure HUMIN stock solution was adjusted with 1.6 M HCl to pH = 2 and EC = 9340 μs/cm. From this, four samples with approximately 25 mL were created. The Al/C ratio of these samples was adjusted using the gibbsite stock suspension to Al/C values of 0.03 ; 0.05 ; 0.075 and 0.1.

Eight pH and EC measurements were performed during 27 days. During this period a few aluminum measurement were carried out one two of the four samples. After day 8 until day 27 five UV-DOM measurements were performed.

3.4. Experiment series 2 (E2.ySz)

For the second series of experiments a HUMIN stock solution and a gibbsite stock suspension of respectively 3 g/L (0.1 mol C/L) and 3.9 g/L (0.05 Al-mol/L) were created. The gibbsite suspension was stirred continuously during sampling to create a homogeneous suspension. The second series of experiments consisted of three experiments differing in Al/C ratio, HUMIN concentration and amount of gibbsite (see Table 3.2). Each experiment consisted of ten samples with differing starting pH in the range 2-8 (pH = 2 ; 2.5 ; 3 ; 3.5 ; 4 ; 4.5 ; 5 ; 6 ; 7 ; 8), the starting pH served as sample number. Alternately a duplicate of the samples was created. The pH was adjusted with 1.6 M and 0.1 M HCl. Samples with a pH deviation of 0.2 or more from the target starting pH were declined and recreated. The declined samples were not discarded but used as extra measurement. A comprehensive overview of the second series of experiments is given in Appendix B.

Table 3.2: Specifs of the second series of experiments

Experiment	HUMIN 3 g/L (mL)	Gibbsite 3.9 g/L (mL)	Total volume (mL)	Al/C	DOM (g/L)	Gibbsite (g/L)
E2.1Sz	30	0	30	0	3.0	0
E2.2Sz	27.25	2.75	30	0.05	2.7	0.35
E2.3Sz	18.75	11.25	30	0.30	1.9	1.45

Nine pH, EC and DOM measurements were performed during three weeks. After approximately nine and eleven weeks from the start the measurements were repeated. Because these results were very similar the results after eleven weeks will not be shown in the results section. During the whole period a few aluminum measurement were performed.

4

Results and Discussion

First the results of the gibbsite only experiment will be discussed in section 4.1. After which the results of HUMIN and the results of HUMIN plus gibbsite experiments will be discussed in section 4.2. The coding used to describe the samples from all the experiments was:

$$Ex.ySz$$

E stands for Experiment, x = series number, y = experiment number, S stand for Sample and z = sample number In experiment series two the sample number equals the starting pH.

The EC measurements that were conducted on all the experiments showed a collective decrease that could not be explained. The measurements did not give an insight in the occurring processes and will therefore be presented in appendix C.

4.1. Gibbsite dissolution and adsorption

The dissolution of gibbsite and the adsorption of H^+ onto gibbsite was modelled (using visual MINTEQ) and experimentally determined. The modelled results are presented in section 4.1.1 and the experimental results are presented in section 4.1.2.

4.1.1. Modelled gibbsite dissolution and adsorption

The adsorption of H^+ onto gibbsite and the dissolution of gibbsite was modelled using Visual MINTEQ (sections 2.2.4 & 2.2.2). The relative contributions of adsorption and dissolution to a H^+ concentration change strongly depend on pH (see figure 4.1). Where below pH_{start} = 3.5 dissolution is the main process of the decrease in H^+ concentration, while above pH_{start} = 3.5 adsorption is relatively more important. At pH = 6 the contribution of dissolution becomes negative because of the formation of $\mathrm{Al(OH)_4}^-$, thus releasing H^+ instead of consuming it.

Although dissolution is the main process at low pH adsorption of H^+ is still quite significant (figure 4.2). Adsorption of H^+ slowly decreases at increasing starting pH up until zero at PZC, pH = 9 (section 2.2.4). Whilst dissolution is prominent at low pH, it decreases fast with increasing starting pH. From this follows that at low pH most Al is released (figure 4.3).

4.1.2. Experimental determination of gibbsite dissolution and adsorption

Experiment E1.1Sz, gibbsite at low pH, gave insight in the dissolution and adsorption behaviour of gibbsite. Figure 4.4 shows the measured pH over time with the modelled equilibrium pH considering both H^+ adsorption and dissolution. It can be seen that the pH of E1.1S4 and E1.1S5 stabilized around the expected modelled equilibrium after approximately 15 days. E1.1S2 and E1.1S3 are close to modelled equilibrium (ΔpH = 0,52 and 0,39 respectively), whereas E1.1S1 was not near to the modelled equilibrium after 41 days (ΔpH = 1,55).

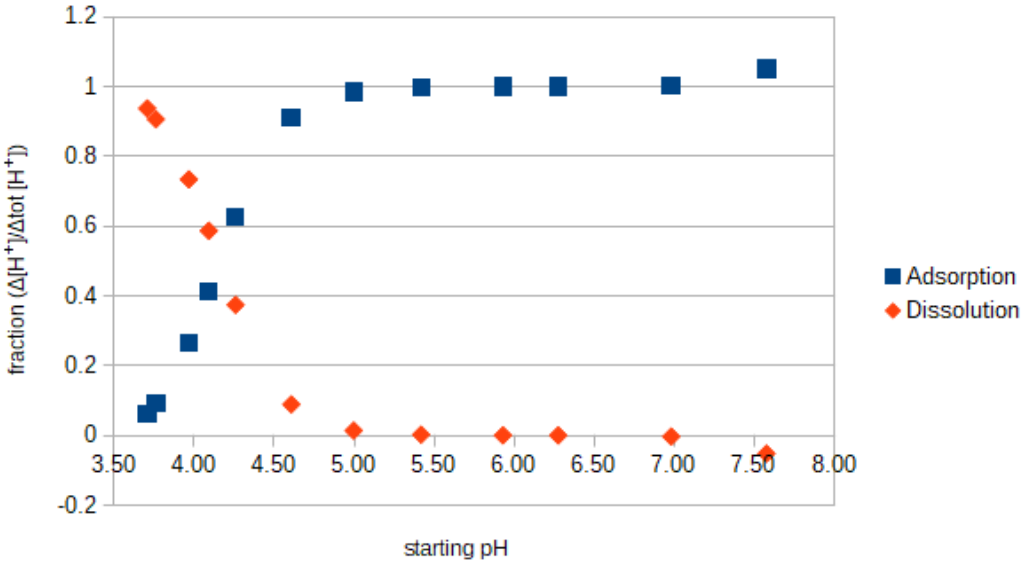

Figure 4.1: Modelled results of the relative distribution of the decrease of H^+ concentration over adsorption and dissolution in relation to starting pH.

From this it appears that the combined adsorption and dissolution rate is faster at the higher initial pH levels, but it must be noted that pH on the y-axis is the H^+ concentration on a logarithmic scale. When the actual H^+ concentration is plotted (see figure 4.5) it is visible that in fact the H^+ 'consumption' is much faster in E1.1S1. This indicates a higher dissolution rate at lower pH.

The results from experiment E1.1Sz confirm the applicability of the model. The results obtained are in good agreement with literature. As Wada and Kakuto (1999) found that at pH_{start} = 3 equilibrium was reached within 120 days. Whereas Su and Harsh (1994) found that at pH_{start} = 2.2 equilibrium was reached after 485 days and at pH_{start} = 1.8 equilibrium was not reached within 861 days. This confirms that the dissolution kinetics are slow and important and a non-equilibrium state can be expected, especially at low pH. From which it can be concluded that gibbsite might only be applicable as a slow but continuous source of Al.

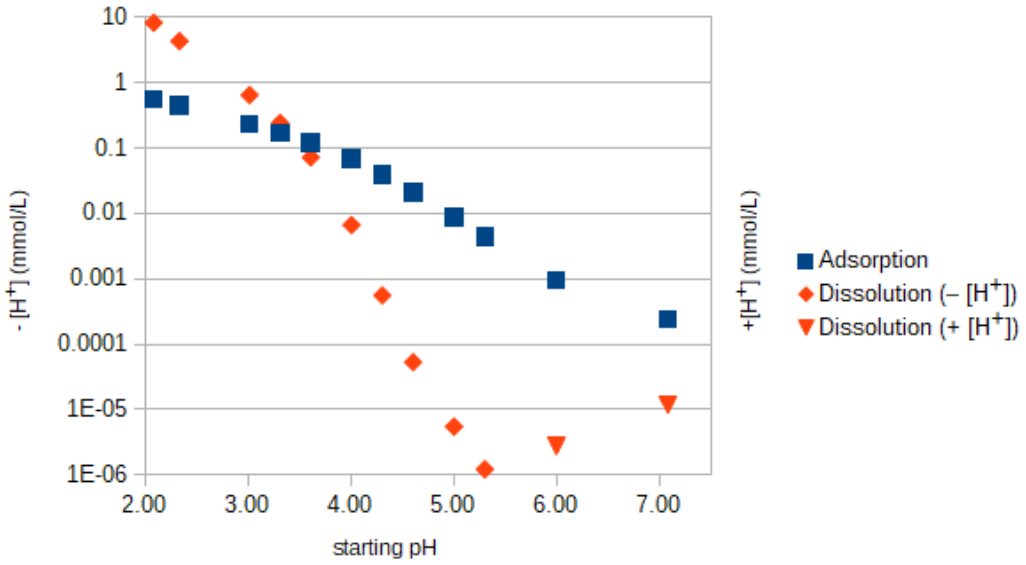

Figure 4.2: Modelled results of the free H^+ concentration change in relation to starting pH. At pH ≥6 dissolution increases the H^+ concentration due to the formation of $Al(OH)_4{}^-$.

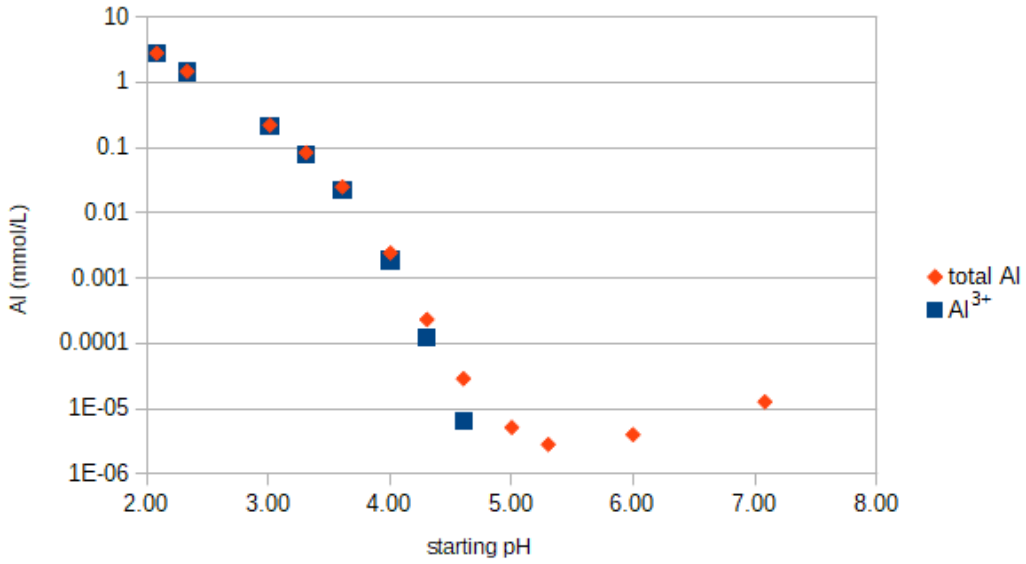

Figure 4.3: Modelled free Al^{3+} and total Al (Al^{3+}, $Al(OH)^{2+}$, $Al(OH)_2{}^+$, $Al(OH)_3$ and $Al(OH)_4{}^-$) concentration in relation to starting pH.

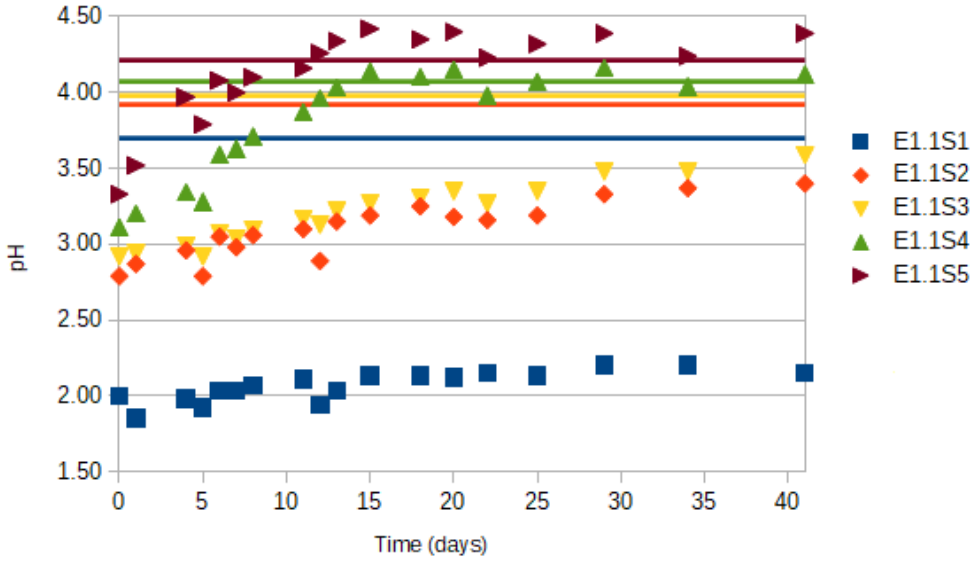

Figure 4.4: Measured pH over time (dots) with the corresponding modelled equilibrium pH considering both adsorption and dissolution (lines).

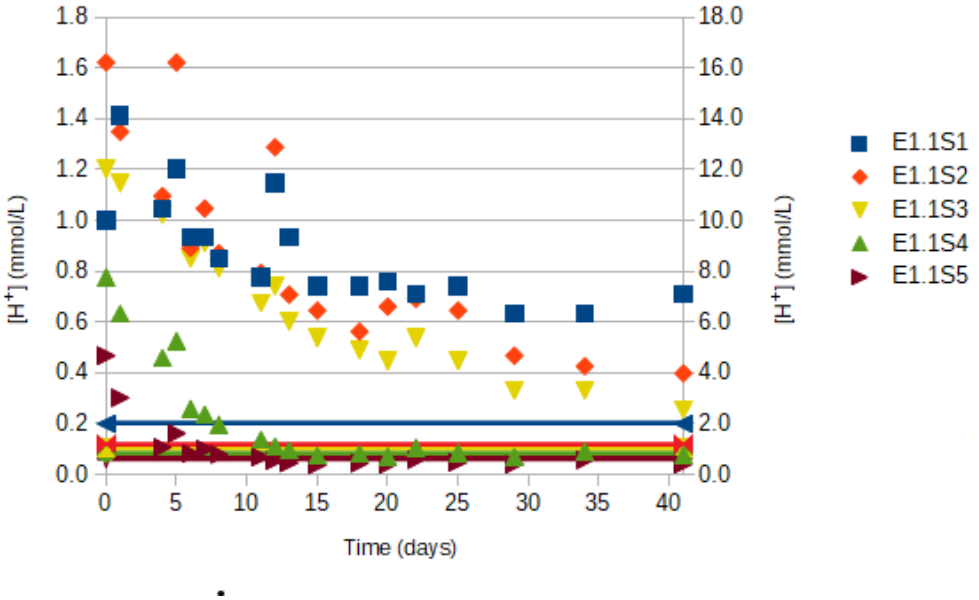

Figure 4.5: The measured H^+ concentration over time (dots) with the corresponding modelled equilibrium pH considering both adsorption and dissolution (lines). E1.1S1 is plotted against the secondary y-axis.

4.2. HUMIN and HUMIN plus gibbsite

The other experiments of series one and the experiments of series two gave insight in the behaviour of HUMIN and of HUMIN with gibbsite at the starting pH range: 2 – 8. The results are presented in sections based on pH-sub-ranges in which similar behaviour was found:

- 4.2.1. Low pH (pH_{start} = 2 - 2.5)
- 4.2.2. Transitional zone (pH_{start} = 3 - 3.5)
- 4.2.3. Neutral to high pH (pH_{start} = 4 - 8)

In each section corresponding colours are used to show the results. The results of the second series of experiments are depicted in yellow (E2.1Sz), red (E2.2Sz) and blue (E2.3Sz), the corresponding HUMIN concentration (H) and amount of gibbsite (G) are included in the captions. Furthermore, data presented within a section with the same symbol has the same starting pH. The results of the first series of experiments are depicted in grey. Alternatively an overview of the specifics of all the samples, that are discussed within the section, are given at the beginning of each section (see tables 4.1, 4.2 and 4.3).

4.2.1. Low pH (pH_{start} = 2 - 2.5)

Table 4.1: Starting pH, final pH with the experimental duration, ΔH^+ concentration, HUMIN concentration and amount of gibbsite of each sample discussed in section 4.2.1

	pH_{start}	pH_{final} (days)	$\Delta[H^+](mmol/L)$	HUMIN (g/L)	Gibbsite (g/L)
E2.1S2	2.00	1.98 (61)	0.47	3.0	-
E2.1S2.5	2.45	2.51 (61)	-0.46	3.0	-
E2.2S2	1.99	2.06 (61)	-1.52	2.7	0.35
E2.2S2.5	2.53	2.70 (61)	-0.96	2.7	0.35
E2.3S2	2.04	2.26 (61)	-3.62	1.9	1.45
E2.3S2.5	2.52	2.81 (61)	-1.47	1.9	1.45
E1.2S2	2.20	2.14 (28)	0.93	3.0	-
E1.2S3	2.52	2.59 (28)	-0.45	3.0	-
E1.3S1	2.03	2.20 (41)	-3.02	2.3	0.60
E1.4S1	1.99	2.15 (27)	-3.15	2.9	0.23
E1.4S2	1.99	2.11 (27)	-2.47	2.9	0.38
E1.4S3	1.99	2.07 (18)	-1.72	2.8	0.54
E1.4S4	1.99	2.12 (27)	-2.65	2.7	0.70

Figure 4.6 shows the measured pH over time of the samples of the second series of experiments with low starting pH and E1.3S1 and E1.4S2. Data from E2.1S2 and E2.1S2.5 illustrate that HUMIN did not significantly affect the pH over time. The results of E1.2S2 and E1.2S3 are not depicted in the figure but showed the same behaviour.

The data of E2.3S2.5, E2.2S3, E2.3S3 and E1.3S1 show that the pH goes up when there is gibbsite involved. This effect was less clear in E2.2S2.5 while E1.4S2 (with similar specifics) did show a slight pH increase. Because HUMIN did not affect the pH over time the pH increase is attributed to adsorption of H^+ onto gibbsite and the dissolution of gibbsite. Furthermore the data shows that at higher amounts of gibbsite the pH increase was higher (amounts of gibbsite are included in figure 4.6).

A higher amount of gibbsite means more adsorption sites for H^+. Although in section 4.1.1 it was concluded that at pH_{start} = 2 the adsorption did not play a major role, it must be noted that it was referring to modelled equilibrium. It was also concluded that reaching equilibrium at low starting pH is a slow process and a non-equilibrium state can be expected. Stumm and Wollast (1990) stated that

adsorption is fast and dissolution is slow. From this it can be concluded that the influence of adsorption at low starting pH cannot be neglected. Furthermore the dissolution rate is enhanced by adsorption (Stumm and Wollast, 1990). The combined influence of adsorption and subsequently an enhanced dissolution rate are expected to be the cause of the higher initial pH increase at higher amounts of gibbsite.

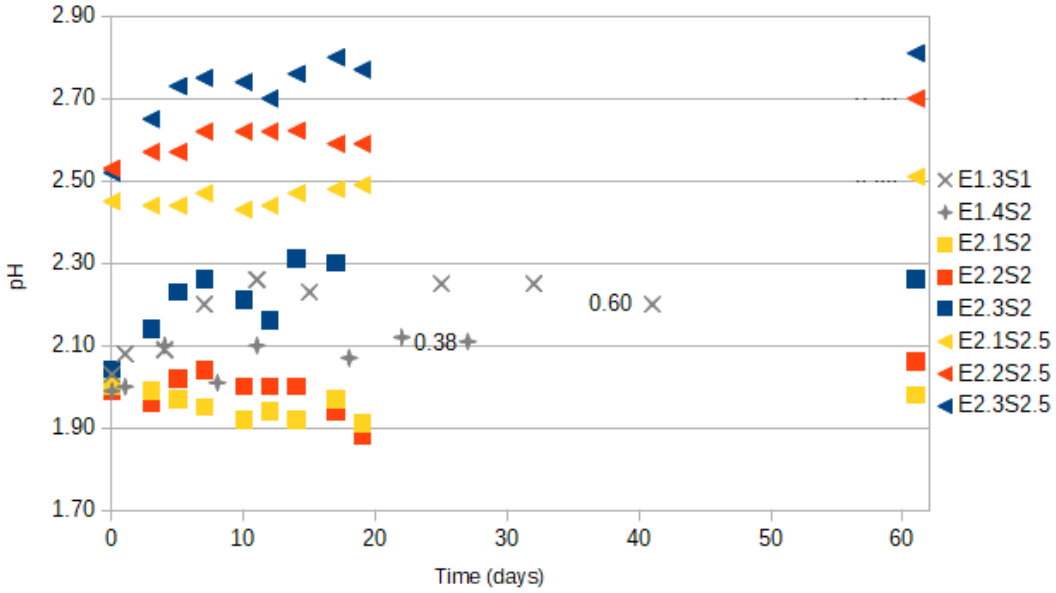

Figure 4.6: pH over time at low starting pH. Yellow: H = 3 g/L, G = 0 g/L; Red: H = 2.7 g/L, G = 0.35 g/L; Blue: H = 1.9 g/L, G = 1.45 g/L. □: pH_{start} = 2 ; ◁: pH_{start} = 2.5. Amount of gibbsite (g/L) of E1.3S1 and E1.4S2 is depicted in graph next to the last measurement point.

Figure 4.8 and figure 4.9 show the normalized measured DOM concentration over time of the samples of the second series of experiments with low starting pH. The first DOM concentration measurement was performed 3 days after sample preparation. It can be seen that most of the HUMIN precipitated before the first measurement. Only a small fraction stayed soluble (3-4%). The stable pH of E2.1S2 and E2.1S2.5 and visual conformation of the quick formation of a clear supernatant (<2hr), indicate that the HUMIN protonated fast during the acidification of the samples and subsequently precipitated. Figure 4.7 shows the clear separation of a precipitation layer and a clear supernatant layer.

Data from E2.3S2.5 show a slight decrease in DOM fraction over time, which can be explained by continuous protonation and subsequent flocculation of the DOM. The small difference in the soluble fractions between the experiments at the end of the experiment could be explained by one or more of the following reasons: 1) different HUMIN concentrations; 2) different ionic strength; 3) formation of soluble $Al{-}DOM$ complexes and 4) difference in pH level. Because the differences are small it is difficult to draw a definite conclusion.

Some Al measurements were done on E2.2S2.5 and E2.3S2.5 during the experiment and one Al measurement was done on E2.2S2 and E2.3S2 at the end of the experiment. The results confirmed the pH dependency of dissolution (more dissolution at lower pH) but could not be fully explained. They are given and discussed more extensively in appendix D.

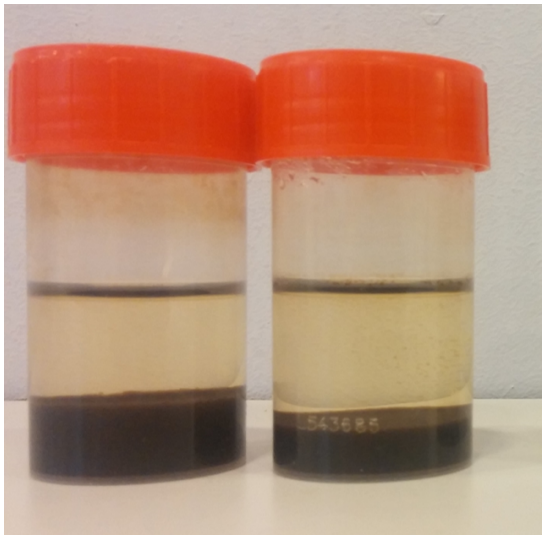

Figure 4.7: Photo of a sample showing the separation of precipitation and supernatant layers.

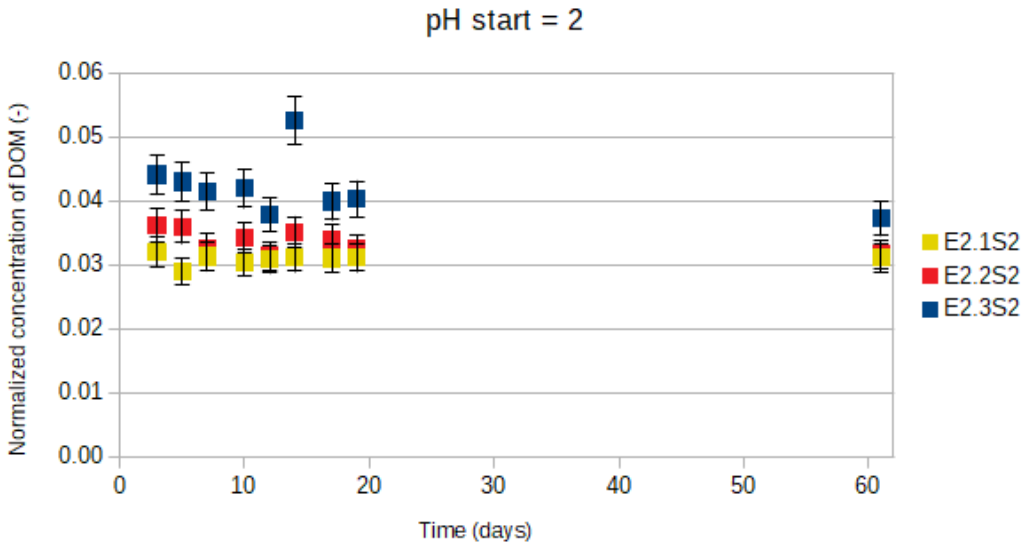

Figure 4.8: DOM concentration normalized to the initial DOM concentration (t_0) over time. Yellow: H = 3 g/L, G = 0 g/L; Red: H = 2.7 g/L, G = 0.35 g/L; Blue: H = 1.9 g/L, G = 1.45 g/L.

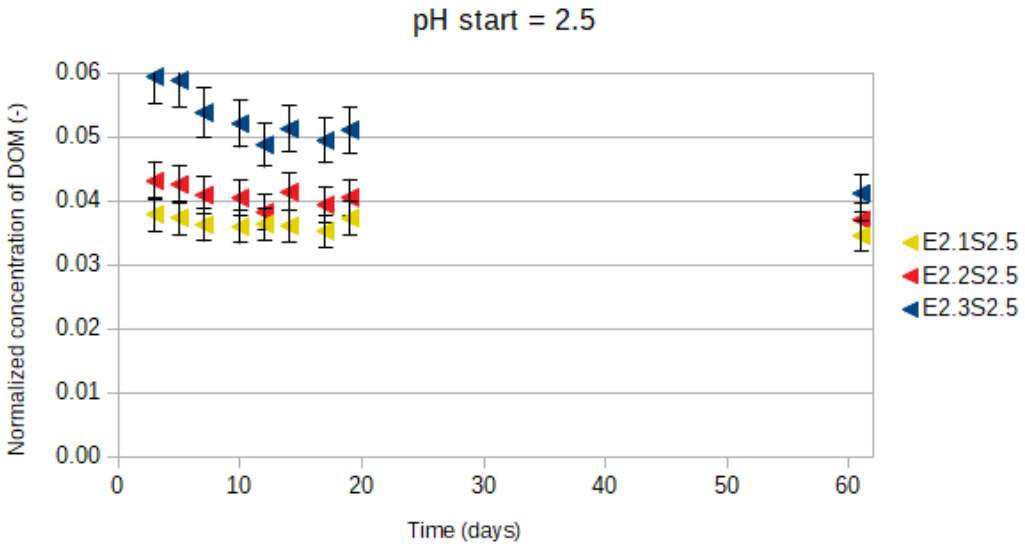

Figure 4.9: DOM concentration normalized to the initial DOM concentration (t_0) over time. Yellow: H = 3 g/L, G = 0 g/L; Red: H = 2.7 g/L, G = 0.35 g/L; Blue: H = 1.9 g/L, G = 1.45 g/L.

4.2.2. Transitional zone (pH_{start} = 3 - 3.5)

Table 4.2: Starting pH, final pH with the experimental duration, ΔH^+ concentration, HUMIN concentration and amount of gibbsite of each sample discussed in section 4.2.2

	pH_{start}	pH_{final} (days)	$\Delta[H^+](mmol/L)$	HUMIN (g/L)	Gibbsite (g/L)
E2.1S3	3.02	3.35 (61)	-0.51	3.0	-
E2.1S3.5	3.60	4.13 (61)	-0.18	3.0	-
E2.2S3	3.08	3.50 (61)	-0.52	2.7	0.35
E2.2S3.5	3.53	4.15 (61)	-0.22	2.7	0.35
E2.3S3	3.03	3.56 (61)	-0.66	1.9	1.45
E2.3S3.5	3.56	4.28 (61)	-0.22	1.9	1.45
E1.1S3	2.92	3.59 (41)	-0.95	-	7.60
E1.1S4	3.11	4.12 (41)	-0.70	-	7.60
E1.1S5	3.33	4.39 (41)	-0.43	-	7.63
E1.2S4	2.98	3.27 (28)	-0.51	±3	-

Figure 4.10 shows the measured pH over time of the samples of the second series experiments with starting pH's: 3 – 3.5 and E1.2S4. In contrast to what was observed at starting pH's 2 – 2.5, experiments E2.1S3, E2.1S3.5 and E1.2S4 show that the pH increases over time when there is no gibbsite involved. This means that the functional groups of HUMIN protonated over time.

The HUMIN concentration in the experiments that included gibbsite (E2.2S3; E2.2S3.5; E2.3S3 and E2.3S3.5) were lower, so a smaller pH increase is expected due to the continuous protonation of HUMIN. Considering that the pH increased stronger in these experiments means that adsorption and dissolution took place.

When compared to E1.1Sz, the gibbsite only experiment described in section 4.1, the pH increase was lower (because E1.1Sz did not have samples starting at exactly 3 or 3.5 it is not possible to give an exact ΔpH, but averaging and extrapolating the results of E1.1Sz gives $\Delta pH_{start\ =\ 3}$ = 0.33 and $\Delta pH_{start\ =\ 3.5}$ = 0.49). This results can be attributed to the lower amount of gibbsite and the presence of HUMIN. The continuous protonation of HUMIN causes competition for H^+ between HUMIN and gibbsite. Consequently, this competition slows the adsorption and, the already slow, dissolution of gibbsite down.

Figure 4.11 and figure 4.12 show the normalized measured DOM concentration over time of the samples of the second series of experiments with starting pH's 3 – 3.5. The results will be discussed per starting pH level.

At starting pH = 3, when there was no gibbsite involved (E2.1S3), the HUMIN almost completely precipitated (95%) before the first measurement started at day 3 (figure 4.11). When gibbsite was involved (E2.2S3 and E2.3S3) a fraction of the HUMIN stayed soluble and precipitated over time. This can be explained by the fact that the protonation has to compete for H^+ with the adsorption and dissolution of gibbsite. Moreover, Al released from gibbsite dissolution has a higher affinity towards HUMIN functional groups than H^+. Given the low Al/C ratio, Al forms soluble $Al{-}DOM$ complexes with HUMIN and this stabilizes the HUMIN. Over time, due to continuous protonation and flocculation (and partly complexation), the DOM still precipitated.

The same phenomena, though delayed, can be seen at starting pH = 3.5 (figure 4.12). Data from E2.1S3.5 show that when there was no gibbsite involved approximately half of the HUMIN precipitated within 3 days, whereas with gibbsite involved (E2.2S3.5 and E2.3S3.5) almost all HUMIN stayed soluble. Over time almost all HUMIN precipitated when there was no gibbsite involved whereas most HUMIN was still soluble with gibbsite involved. This can once again be explained by the competition for

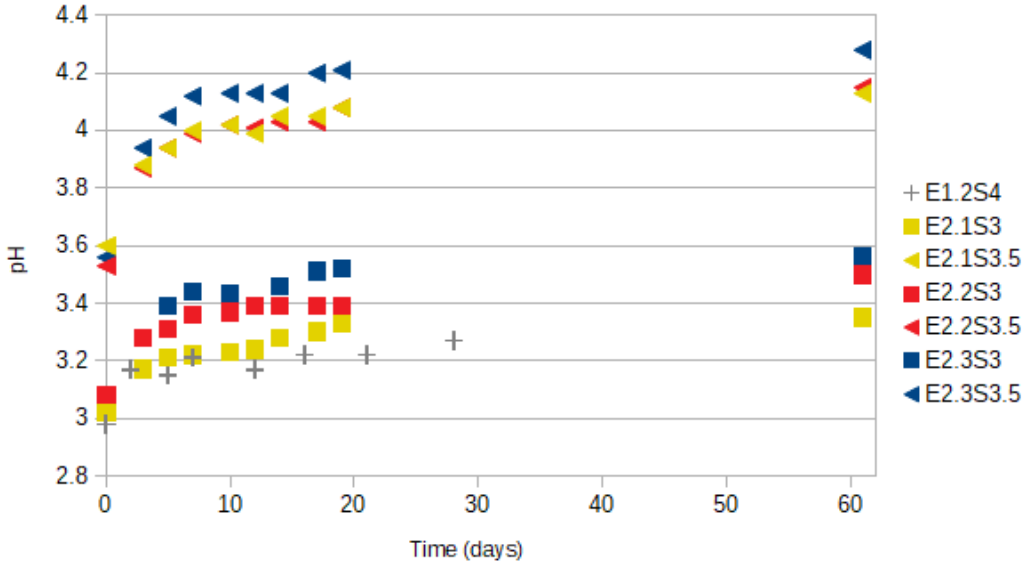

Figure 4.10: pH over time in transitional zone. Yellow: H = 3 g/L, G = 0 g/L; Red: H = 2.7 g/L, G = 0.35 g/L; Blue: H = 1.9 g/L, G = 1.45 g/L. □: pH_{start} = 3 ; ◁: pH_{start} = 3.5. E1.2S4: H = ±3 g/L, G = 0 g/L.

H^+ and the formation of soluble $Al-DOM$ complexes as described earlier. Besides, during the experiment the pH in E2.2S3.5 and E2.3S3.5 was also higher than E2.1S3.5 (figure 4.10) making protonation less likely and DOM more stable.
Some Al measurements were done on E2.2S3, E2.2S3.5, E2.3S3 and E2.3S3.5. The results confirmed the pH dependency of dissolution (more dissolution at lower pH) but could not be fully explained. They are given and discussed more extensively in appendix D.

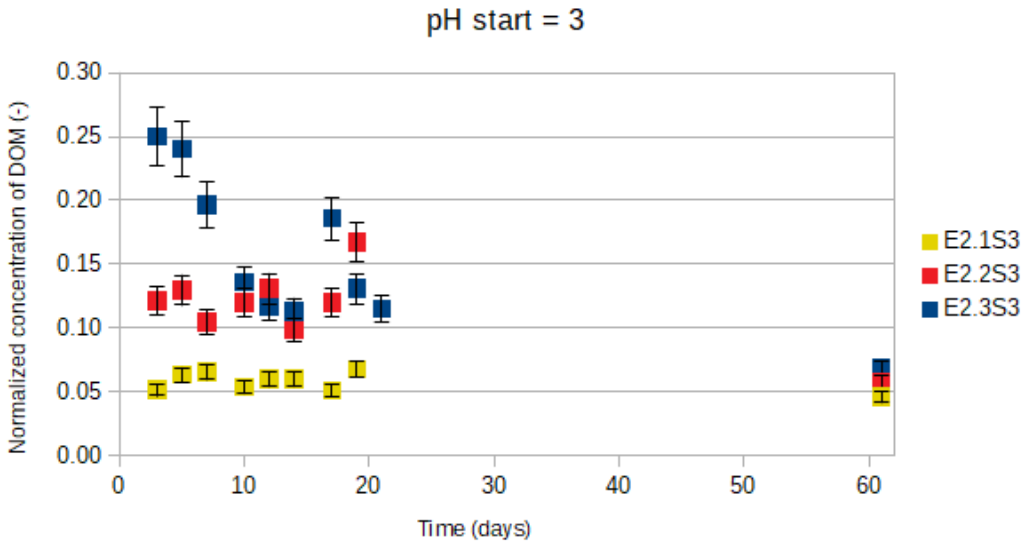

Figure 4.11: DOM concentration normalized to the initial DOM concentration (t_0) over time. Yellow: H = 3 g/L, G = 0 g/L; Red: H = 2.7 g/L, G = 0.35 g/L; Blue: H = 1.9 g/L, G = 1.45 g/L.

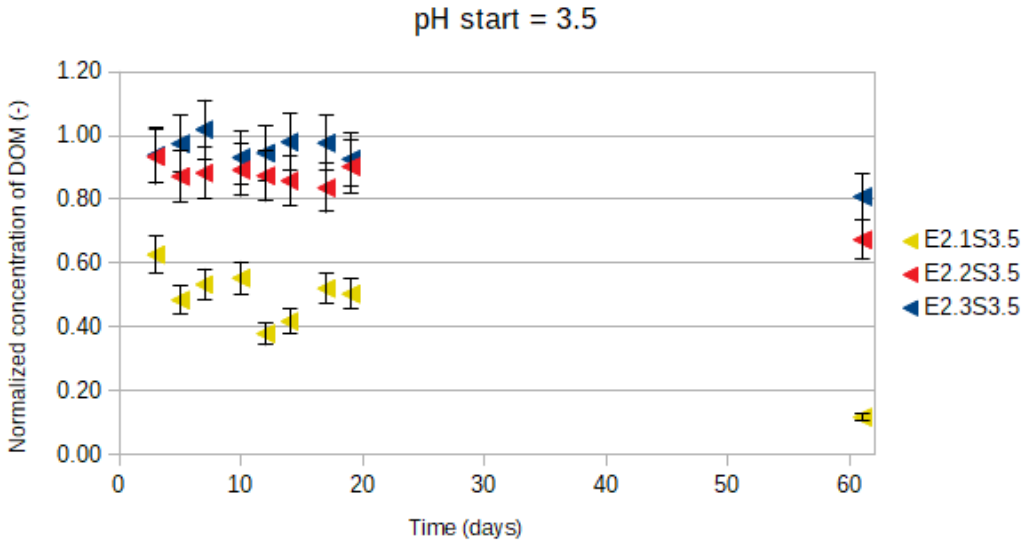

Figure 4.12: DOM concentration normalized to the initial DOM concentration (t_0) over time. Yellow: H = 3 g/L, G = 0 g/L; Red: H = 2.7 g/L, G = 0.35 g/L; Blue: H = 1.9 g/L, G = 1.45 g/L.

4.2.3. Neutral to high pH (pH_{start} = 4 - 8)

Table 4.3: Starting pH, final pH with the experimental duration, ΔH^+ concentration, HUMIN concentration and amount of gibbsite of each sample discussed in section 4.2.3

	pH_{start}	pH_{final} (days)	$\Delta[H^+](mmol/L)$	HUMIN (g/L)	Gibbsite (g/L)
E2.1S4 -4	4.07	4.83 (61)	-0.07	3.0	-
E2.1S4.5	4.50	5.30 (61)	-0.03	3.0	-
E2.1S5	5.02	5.92 (61)	-0.01	3.0	-
E2.1S6	6.02	7.21 (61)	-0.00	3.0	-
E2.1S7	7.02	7.70 (61)	-0.00	3.0	-
E2.1S8	8.02	8.19 (61)	-0.00	3.0	-
E2.2S4	3.98	4.67 (61)	-0.08	2.7	0.35
E2.2S4.5	4.45	5.23 (61)	-0.03	2.7	0.35
E2.2S5 -2	5.00	5.84 (61)	-0.01	2.7	0.35
E2.2S6	6.06	7.27 (61)	-0.00	2.7	0.35
E2.2S7	7.08	7.77 (61)	-0.00	2.7	0.35
E2.2S8	8.10	7.95 (61)	0.00	2.7	0.35
E2.3S4	4.03	4.85 (61)	-0.08	1.9	1.45
E2.3S4.5 -2	4.52	5.40 (61)	-0.03	1.9	1.46
E2.3S5 -2	4.99	5.98 (61)	-0.01	1.9	1.46
E2.3S6	6.05	7.32 (61)	-0.00	1.9	1.43
E2.3S7	7.01	7.74 (61)	-0.00	1.9	1.45
E2.3S8	8.03	7.88 (61)	0.00	1.9	1.46
E1.3S3	4.01	4.83 (41)	-0.08	2.6	0.67
E1.3S4	5.00	5.84 (41)	-0.01	2.6	0.68
E1.3S5	5.99	6.95 (41)	-0.00	2.7	0.69
E1.3S6	6.97	7.53 (41)	-0.00	2.7	0.70
E1.3S7	8.07	7.68 (41)	0.00	2.7	0.70
E1.3S8	8.71	7.99 (41)	0.00	2.7	0.71

Figure 4.13 and figure 4.14 show the measured pH over time of the samples of the second series of experiments and E1.3Sz with neutral to high starting pH. To give a clear overview, the pH range is given in two smaller pH ranges, pH_{start} = 4 – 5 (figure 4.13) and pH_{start} = 6 – 8 (figure 4.14).

It can be seen that for all experiments within the starting pH range 4 – 7 the pH increased strongly in the first ten days after which the pH stabilized. No trend difference between excluding or including gibbsite can be found. This means that adsorption and dissolution did not happen significantly and the pH increase can be attributed solely to the continuous protonation of HUMIN. With increasing starting pH less continuous protonation of HUMIN happened.

E2.1S8, E2.2S8 and E2.3S8 (starting pH = 8) did not show this clear pH increase, indicating that at this pH no protonation over time happened. An interesting small pH difference was found at the end of the experiment between excluding and including gibbsite. This difference implies that a small amount of gibbsite dissolved to $Al(OH)_4^-$, thereby slightly lowering the pH. This process was found more clearly in E1.3S7 and unmistakeably in E1.3S8.

Figure 4.15 shows the normalized measured DOM concentration over time of the samples of E2.1Sz with neutral to high starting pH. It can be seen that the HUMIN stayed soluble over time over the whole pH range. E2.2Sz and E2.3Sz showed the same results (appendixes E and F). Differences between samples and experiments cannot be addressed with any reliability as a dilution factor of 40x was needed to perform the DOM measurements.

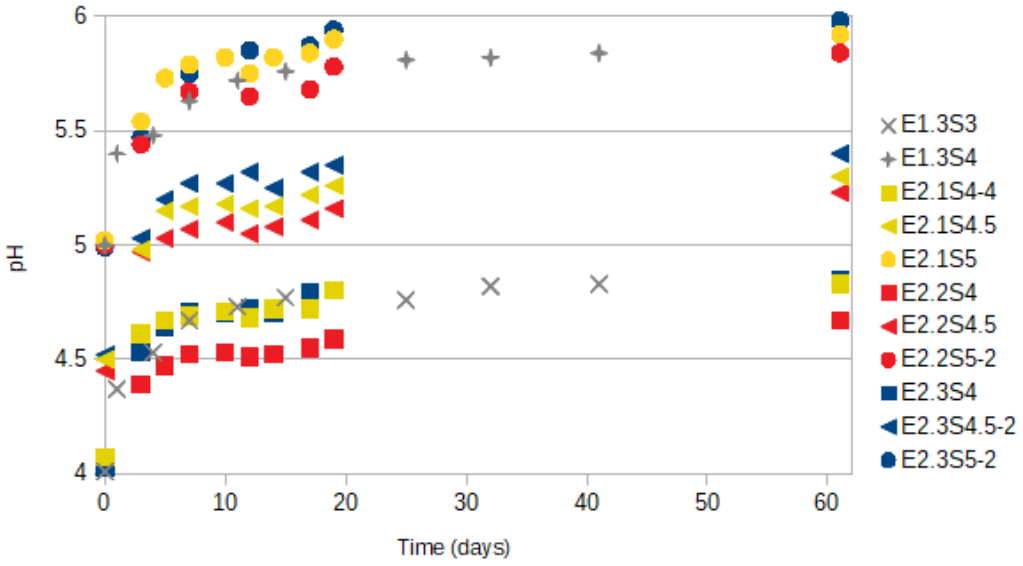

Figure 4.13: pH over time at neutral to high pH. Yellow: H = 3 g/L, G = 0 g/L; Red: H = 2.7 g/L, G = 0.35 g/L; Blue: H = 1.9 g/L, G = 1.45 g/L; grey: H = 2.6 g/L, G = ±0.7 g/L. □: pH_{start} = 4; ◁: pH_{start} = 4.5; ○: pH_{start} = 5.

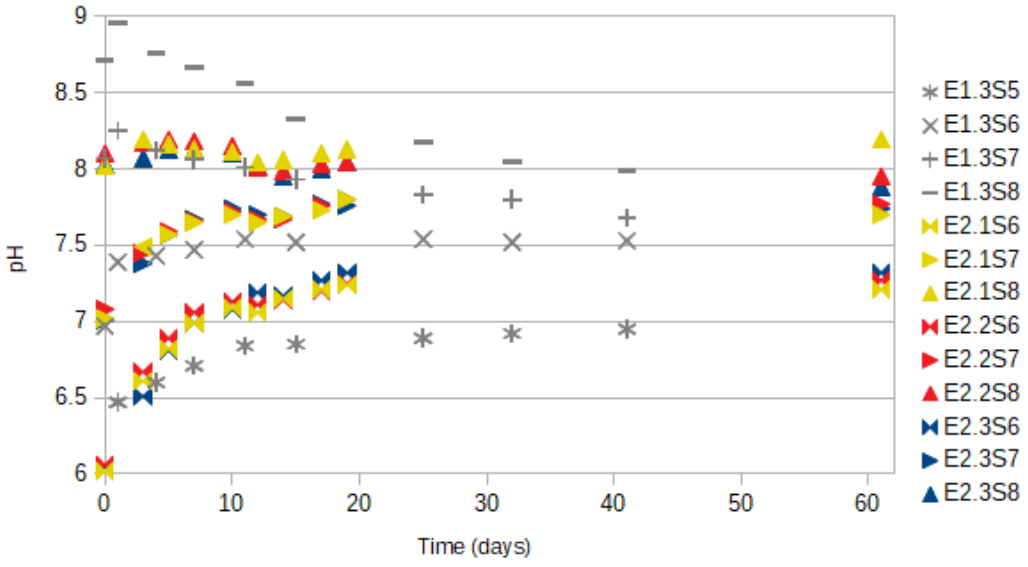

Figure 4.14: pH over time at neutral to high pH. Yellow: H = 3 g/L, G = 0 g/L; Red: H = 2.7 g/L, G = 0.35 g/L; Blue: H = 1.9 g/L, G = 1.45 g/L; grey: H = 2.6 g/L, G = ±0.7 g/L. ⋈: pH_{start} = 6; ▷: pH_{start} = 7; △: pH_{start} = 8.

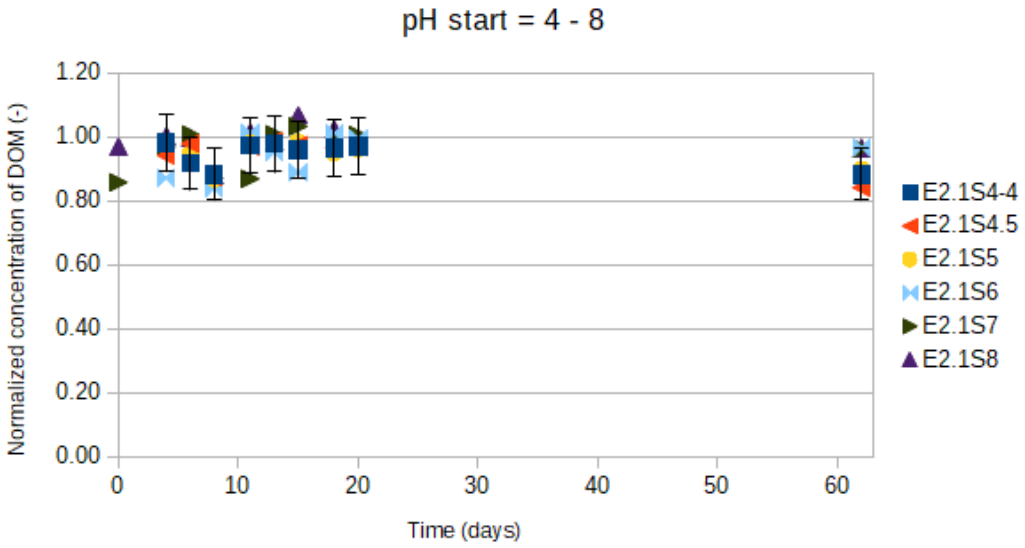

Figure 4.15: DOM concentration normalized to the initial DOM concentration (t_0) of E2.1Sz over time.

5

Conclusion and Outlook

The goal of this research was to investigate if gibbsite can be used as aluminum source to complex and precipitate with organic matter in the interest of soil permeability reduction.

To achieve this goal a literature study was conducted in combination with 2 series of experiments. The results of the experiments were:

- At low pH (pH = 2 - 2.5) the protonation, flocculation and subsequently precipitation of HUMIN was the dominant (fast) process whereas gibbsite dissolution was the dominant (slow) process. Both processes happened subsequently, eliminating the chance of significant complexation.
- In the transitional zone (pH = 3 - 3.5) the competition for H^+ between HUMIN and gibbsite was predominant. Thereby increasing the stability of DOM and slowing down the dissolution of gibbsite, giving the possibility of complexation.
- At neutral to high pH HUMIN (pH = 4 - 8) protonated over time but did not precipitate (or considerably adsorb to gibbsite). No significant adsorption or dissolution of gibbsite was found below starting pH = 8, but at pH ≥ 8 gibbsite dissolution to $Al(OH)_4^-$ was indicated.

This research did not directly show that gibbsite can be used as aluminum source to complex and precipitate with organic matter, mainly because of:

1. The separation of gibbsite dissolution and soluble HUMIN in time
2. The slow kinetics of gibbsite dissolution.

1. The separation of gibbsite dissolution and HUMIN stability might be coped with in the following ways:

- Lowering 'the transitional' pH, by using an OM source richer in fulvic acids. This way the OM is soluble at lower pH increasing the overlap at which gibbsite dissolves and OM is still soluble.
- Literature and experimental data in this research point out that gibbsite dissolves at high pH (to $Al(OH)_4^-$). A mixture of gibbsite and OM at high pH and at equilibrium would give $Al(OH)_4^-$ and soluble OM. By suddenly dropping the pH to acidic conditions, $Al(OH)_4^-$ is (partly) converted to Al^{3+} which subsequently can complex with the DOM.
- A gibbsite suspension at a low pH at equilibrium would give Al^{3+}. If the suspension is mixed with DOM (at high pH), both species will (partly) complex, as complexation is fast and gibbsite precipitation relatively slow.

The first option is a good practical suggestion. Whereas the other two suggestions would be interesting to investigate (especially the dissolution of gibbsite at high pH and the transformation of $Al(OH)_4^-$ to Al^{3+}). However, to obtain sufficient Al a very low or high pH is needed and on top of that it takes a long time to reach equilibrium. It seems therefore that these options are impractical to apply in practise.

Nonetheless, both suggestions might be applicable to create partly amorphous gibbsite. Using them as pretreatment would yield gibbsite with a higher (starting) solubility.

2. The slow kinetics of gibbsite are hard to change. From literature it was found that the dissolution rate increases with increasing temperature, but in practise it will be difficult to obtain high temperatures for a long period. Furthermore, it was found that gibbsite dissolution at low pH is was controlled by reactions at the solid-solution interface. This means that gibbsite with a high surface area dissolves faster. Moreover, literature showed that natural gibbsite is more soluble than synthetic gibbsite, which was used in this research. Instead of significantly changing the slow kinetics of gibbsite it could be used, by looking at bigger time-scales. In the transitional zone gibbsite did dissolve but slowly, therefore creating soluble $\mathrm{Al{-}DOM}$ complexes (because the Al/C was low). However, over time the Al/C will increase thereby saturating the complexes until they precipitate. This slow Al release and subsequent precipitation could be used in robust problems that require a self healing ability.

For the implementation of gibbsite, as aluminum source to complex and precipitate with organic matter, it is needed to look at robust problems that require a slow release of Al and investigate the use of natural gibbsite sources with preferably high surface areas.

Advice
It is advised to continue the research on gibbsite as aluminum source. This research should include trustworthy free aluminum measurements. Furthermore it is advised to use a fulvic acid rich OM source and a pretreated natural gibbsite source.

A elementary practical design, closely based on the podzolization process, is proposed and given in figure 5.1. An acidic DOM layer is constructed above a gibbsite layer. The acidic DOM slowly leaches through the gibbsite thereby dissolving the gibbsite. The Al and DOM form soluble complexes with downward increasing Al saturation. At the buffer layer (for example $\mathrm{CaCO_3}$) the soluble complexes become unstable and precipitate, forming a low permeability layer. It must be noted that $\mathrm{CaCO_3}$ can dissolve thus (partly) cancelling permeability reduction by complexation.

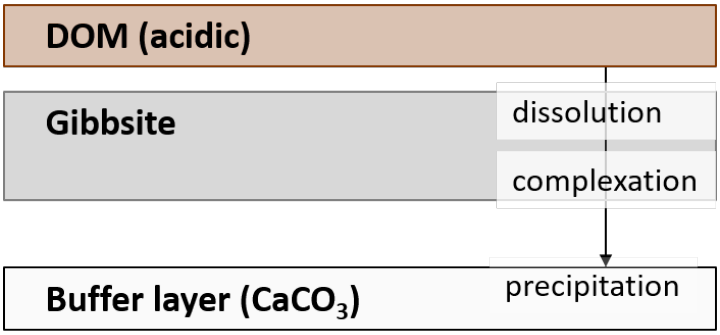

Figure 5.1: Schematic overview of a possible design with the implementation of gibbsite as aluminum source.

Experimental recommendations

In short a simple, almost obvious, advice is given: keep everything constant except the parameter(s) that you want to research.

It was found in literature that the ionic strength influenced all occurring processes in this thesis. It is therefore advised to use a background electrolyte in further research to obtain a constant ionic strength and therefore eliminate the influence of ionic strength on the results. Problems arise at extreme pH levels, as the addition of acids/bases affects the ionic strength (Lützenkirchen et al., 2012). But this could be cooped with using a high ionic strength background electrolyte and accurate free proton measurements (Lützenkirchen et al., 2002).

Furthermore it is advised to use corresponding DOM concentrations or amounts of gibbsite, to increase the comparability between experiments.

It is difficult to take homogeneous samples from a suspension. It is therefore advised to not make use of (gibbsite) stock suspension when creating samples but weigh the input for each sample. When using this procedure precise scales are needed as it is likely very small gibbsite input per sample is needed. If such scales are not available it is important to keep the stock solutions as homogeneous as possible by continuous stirring during sampling.

Bibliography

P. R. Bloom. The Kinetics of Gibbsite Dissolution in Nitric Acid. *Soil Science Society of America Journal*, 47:164–168, 1983. doi: 10.2136/sssaj1983.03615995004700010032x. URL http://dx.doi.org/10.2136/sssaj1983.03615995004700010032x.

Chiara Bonfiglo. Hydraulic conductivity reduction induced by precipitation of aluminium-organic matter flocs in porous media. 2016.

P. Buurman and A. G. Jongmans. Podzolisation and soil organic matter dynamics. *Geoderma*, 125 (1-2):71–83, 2005. ISSN 00167061. doi: 10.1016/j.geoderma.2004.07.006.

William T. Choate and John A. S. Green. U.S. Aluminum Production Energy Requirements: Historical Perspective, Theoretical Limits, and New Opportunities. *ACEEE Summer Study on Energy Efficiency in Industry*, pages 12–24, 2003.

Nicholas Clarke and Lars Göran Danielsson. The simultaneous speciation of aluminium and iron in a flow-injection system. *Analytica Chimica Acta*, 306(1):5–20, 1995. ISSN 00032670. doi: 10.1016/0003-2670(94)00674-B.

James A. Davis and James O. Leckie. Effect of Adsorbed Complexing Ligands on Trace Metal Uptake by Hydrous Oxides. *Environmental Science and Technology*, 12(12):1309–1315, 1978. ISSN 15205851. doi: 10.1021/es60147a006.

Jack de Ruiter. Principles of Drug Action 1: Resonace and Induction Tutorial. *Principles of Drug Action 1*, pages 1–19, 2005a.

Jack de Ruiter. Carboxylic Acid Structure and Chemistry: Part 1. *Principles of Drug Action 1*, pages 1–11, 2005b.

B. Deflandre and Jean Pierre Gagné. Estimation of dissolved organic carbon (DOC) concentrations in nanoliter samples using UV spectroscopy. *Water Research*, 35(13):3057–3062, 2001. ISSN 00431354. doi: 10.1016/S0043-1354(01)00024-0.

J. B. Dixon and S. B. Weed. *Minerals in soil environments*. Soil science society of america, Madison, 1977.

Jinming Duan and John Gregory. Coagulation by hydrolysing metal salts. *Advances in Colloid and Interface Science*, 100-102(SUPPL.):475–502, 2003. ISSN 00018686. doi: 10.1016/S0001-8686(02)00067-2.

David A. Dzombak and François Morel. *Surface complexation modeling : hydrous ferric oxide*. New York : Wiley, 1990. ISBN 0471637319.

C. Ekberg and P. L. Brown. *Hydrolysis of Metal Ions*. Wiley-VCH, Weinheim, 2016. URL https://books.google.nl/books?id=LO6hCwAAQBAJ&pg=PT1036&lpg=PT1036&dq=Al13(OH)327%2B+or+Al13+O4+(OH)247%2B&source=bl&ots=lzddehYabQ&sig=-U3fnWrusGnL3GtQc994kf9v_bI&hl=nl&sa=X&ved=0ahUKEwj4sKml6d7XAhVIuBoKHYzzD4kQ6AEIJzAA#v=onepage&q=Al13(OH)327%2BorAl13.

K. Eusterhues, A. Hädrich, J. Neidhardt, K. Küsel, T. F. Keller, K. D. Jandt, and K. U. Totsche. Reduction of ferrihydrite with adsorbed and coprecipitated organic matter: Microbial reduction by Geobacter bremensis vs. abiotic reduction by Na-dithionite. *Biogeosciences*, 11(18):4953–4966, 2014. ISSN 17264189. doi: 10.5194/bg-11-4953-2014.

Cynthia R. Evanko and David A. Dzombak. Influence of structural features on sorption of NOM-analogue organic acids to goethite. *Environmental Science and Technology*, 32(19):2846–2855, 1998. ISSN 0013936X. doi: 10.1021/es980256t.

C. R. Frink and Michael Peech. The solubility of Gibbsite in Aqueous Solutions and Soil Extracts. *Soil Science Society of America Journal*, 26(4):346–347, 1962.

Jiwchar Ganor, Jose Luis Mogollón, and Antonio C Lasaga. Kinetics of gibbsite dissolution under low ionic strength conditions. *Geochimica et Cosmochimica Acta*, 63(11):1635–1651, 1999. ISSN 0016-7037. doi: https://doi.org/10.1016/S0016-7037(99)00069-1. URL http://www.sciencedirect.com/science/article/pii/S0016703799000691.

J. Gregory. *Particles in water*. 2005. ISBN 0203508459. doi: 10.1002/anie.200685451. URL http://discovery.ucl.ac.uk/1300855/.

Henrik Grénman, Tapio Salmi, Dmitry Yu Murzin, and Jonas Addai-Mensah. Dissolution of boehmite in sodium hydroxide at ambient pressure: Kinetics and modelling. *Hydrometallurgy*, 102(1-4):22–30, 2010. ISSN 0304386X. doi: 10.1016/j.hydromet.2010.01.005.

Xiao Hong Guan, Guang Hao Chen, and Chii Shang. Combining kinetic investigation with surface spectroscopic examination to study the role of aromatic carboxyl groups in NOM adsorption by aluminum hydroxide. *Journal of Colloid and Interface Science*, 301(2):419–427, 2006a. ISSN 00219797. doi: 10.1016/j.jcis.2006.05.031.

Xiao Hong Guan, D. L. Li, C. Shang, and Guang Hao Chen. Role of carboxylic and phenolic groups in NOM adsorption on minerals: A review. *Water Science and Technology: Water Supply*, 6(6):155–164, 2006b. ISSN 16069749. doi: 10.2166/ws.2006.959.

Xiao Hong Guan, Chii Shang, and Guang Hao Chen. ATR-FTIR investigation of the role of phenolic groups in the interaction of some NOM model compounds with aluminum hydroxide. *Chemosphere*, 65(11):2074–2081, 2006c. ISSN 00456535. doi: 10.1016/j.chemosphere.2006.06.048.

Hach. Working procedure LCK301 Aluminium, 2013. URL https://uk.hach.com/aluminum-cuvette-test-0-02-0-5-mg-l-al/product-downloads?id=26370269009.

Hach. Aluminum Chromazurol S Method, 2017. URL https://www.hach.com/pipette-variable-volume-1-0-5-0-ml/product-downloads?id=7640438315.

Kristoffer Hagvall, Per Persson, and Torbjörn Karlsson. Speciation of aluminum in soils and stream waters: The importance of organic matter. *Chemical Geology*, 417:32–43, 2015. ISSN 00092541. doi: 10.1016/j.chemgeo.2015.09.012. URL http://dx.doi.org/10.1016/j.chemgeo.2015.09.012.

P. L. Hayden and A. J. Rubin. Systematic investigation of the hydrolysis and precipitation of aluminum (III). *Aqueous-Environmental Chemistry of Metals*, pages 317–381, 1974.

Bruce. S. Hemingway and Garrison Sposito. Inorganic aluminum-bearing solid phases. In *The Environmental Chemistry of Aluminum*, chapter 3, pages 81–116. 1996.

Wesley G. Holtz. Soil as an Engineering Material Engineering. *Journal of Materials*, 1974.

J. Hopman. First insights into Al-OM complexation and the effect of Al-OM flocs on porous mediapermeability. *Delft University of Technology Bachelor Thesis*, (July), 2016.

Pa Ho Hsu. Aluminum hydroxides and oxyhydroxides. In *Minerals in Soil Environments*, pages pp. 99–143. Soil Science Society of America, 1977.

Boris Jansen, Klaas G. J. Nierop, and Jacobus M. Verstraten. Influence of pH and metal/carbon ratios on soluble organic complexation of Fe(II), Fe(III) and Al(III) in soil solutions determined by diffusive gradients in thin films. *Analytica Chimica Acta*, 454(2):259–270, 2001. ISSN 00032670. doi: 10.1016/S0003-2670(01)01551-3.

Boris Jansen, Klaas G. J. Nierop, and Jacobus M. Verstraten. Mobility of Fe(II), Fe(III) and Al in acidic forest soils mediated by dissolved organic matter: Influence of solution pH and metal/organic carbon ratios. *Geoderma*, 113(3-4):323–340, 2003. ISSN 00167061. doi: 10.1016/S0016-7061(02)00368-3.

Boris Jansen, Klaas G. J. Nierop, and Jacobus M. Verstraten. Mechanisms controlling the mobility of dissolved organic matter, aluminium and iron in podzol B horizons. *European Journal of Soil Science*, 56(4):537–550, 2005. ISSN 1365-2389. doi: 10.1111/j.1365-2389.2004.00686.x. URL http://dx.doi.org/10.1111/j.1365-2389.2004.00686.x.

Athanasios K. Karamalidis and David A. Dzombak. *Surface complexation modeling: gibbsite*. 2010. URL https://books.google.nl/books?id=XULsOFSipsgC&pg=PA63&lpg=PA63&dq=Surface+complexation+modeling:+Gibbsite+torrent&source=bl&ots=gta3h8_c0D&sig=-dbwqzknlvst3hiKDDo4Clx4EVw&hl=nl&sa=X&ved=0ahUKEwj6j_-M3Z3aAhVE6aQKHUCoCfIQ6AEIaDAH#v=onepage&q=Schoen&f=false.

H. Kodama, M. Schnitzer, and M. Jaakkimainen. Chlorite and biotite weathering by fulvic acid solutions in closed and open systems. *Canadian Journal of Soil Science*, 63(3):619–629, 1983. doi: 10.4141/cjss83-062. URL https://doi.org/10.4141/cjss83-062.

Ralf König. Validation of cuvette tests for drinking water analysis. Technical report, Hach Lange, 2007.

Gregory V. Korshin, Mark M. Benjamin, and Ronald S. Sletten. Adsorption of natural organic matter (NOM) on iron oxide: Effects on NOM composition and formation of organo-halide compounds during chlorination. *Water Research*, 31(7):1643–1650, 1997. ISSN 00431354. doi: 10.1016/S0043-1354(97)00007-9.

Dileep Kumar, a.P. Singh, P. Raha, Amitava Rakshit, C.M. Singh, and P. Kishor. Potassium Humate: A Potential Soil Conditioner and Plant Growth Promoter. *International Journal of Agriculture, Environment and Biotechnology*, 6(3):441, 2013. ISSN 0974-1712. doi: 10.5958/j.2230-732X.6.3.015. URL http://www.indianjournals.com/ijor.aspx?target=ijor:ijaeb&volume=6&issue=3&article=015.

Susanne Laumann, Jiani Zhou, and Timo Heimovaara. Groundwater monitoring - SoSEAL pilot Veersedijk. pages 1–9, 2016.

Boris Levinsky. Humates and Humic Acids, How do they work? *Teravita*, 1:1–24, 2008. URL http://www.hoodridge.com/media/humatesandhumicacids.pdf.

Willard Lyman Lindsay. *Chemical equilibria in soils*. Colorado State University, Fort Collins, 1979.

Ulla S. Lundström, N. Van Breemen, and D. Bain. The podzolization process. A review. *Geoderma*, 94(2-4):91–107, 2000a. ISSN 00167061. doi: 10.1016/S0016-7061(99)00036-1.

Ulla S. Lundström, N. Van Breemen, D. C. Bain, P. A.W. Van Hees, R. Giesler, J. P. Gustafsson, H. Ilvesniemi, E. Karltun, P. A. Melkerud, M. Olsson, G. Riise, O. Wahlberg, A. Bergelin, K. Bishop, R. Finlay, A. G. Jongmans, T. Magnusson, H. Mannerkoski, A. Nordgren, L. Nyberg, M. Starr, and L. Tau Strand. Advances in understanding the podzolization process resulting from a multidisciplinary study of three coniferous forest soils in the Nordic Countries. *Geoderma*, 94(2-4):335–353, 2000b. ISSN 00167061. doi: 10.1016/S0016-7061(99)00077-4.

Johannes Lützenkirchen, Jean François Boily, Lars Lövgren, and Staffan Sjöberg. Limitations of the potentiometric titration technique in determining the proton active site density of goethite surfaces. *Geochimica et Cosmochimica Acta*, 66(19):3389–3396, 2002. ISSN 00167037. doi: 10.1016/S0016-7037(02)00948-1.

Johannes Lützenkirchen, Tajana Preočanin, Davor Kovačević, Vladislav Tomišić, Lars Lövgren, and Nikola Kallay. Potentiometric Titrations as a Tool for Surface Charge Determination. *Croatica Chemica Acta*, 85(4):391–417, 2012. ISSN 00111643. doi: 10.5562/cca2062. URL http://hrcak.srce.hr/file/138013.

Espen Lydersen. The Solubility and Hydrolysis of Aqueous Aluminium Hydroxides in Dilute Fresh Waters at Different Temperatures. *Nordic Hydrology*, 21(3):195–204, 1990. ISSN 00291277.

B. Manunza, C. Gessa, S. Deiana, and R. Rausa. A normal distribution model for the titration curves of humic acids. *Journal of Soil Science*, 43(1):127–131, 1992. doi: 10.1111/j.1365-2389.1992.tb00124.x. URL https://onlinelibrary.wiley.com/doi/abs/10.1111/j.1365-2389.1992.tb00124.x.

R. Bruce Martin. Fe3+ and Al3+ hydrolysis equilibria. Cooperativity in Al3+ hydrolysis reactions, 1991. ISSN 01620134.

Howard M. May, Philip A. Helmke, and Marion L. Jackson. Gibbsite solubility and thermodynamic properties of hydroxy-aluminum ions in aqueous solution at 25°C. *Geochimica et Cosmochimica Acta*, 43(6):861–868, 1979. ISSN 00167037. doi: 10.1016/0016-7037(79)90224-2.

J. A. McKeague, G. J. Ross, and D. S. Gamble. Properties, criteria of classification and genesis of podzolic soils in Canada. *Quaternary Soils*, pages 27–60., 1978.

F. L. Motta, B. A.G. Melo, and M. H.A. Santana. Deprotonation and protonation of humic acids as a strategy for the technological development of pH-responsive nanoparticles with fungicidal potential. *New Biotechnology*, 33(6):773–780, 2016. ISSN 18764347. doi: 10.1016/j.nbt.2016.07.003.

K. L. Nagy and A. C. Lasaga. Dissolution and precipitation kinetics of gibbsite at 80°C and pH 3: The dependence on solution saturation state. *Geochimica et Cosmochimica Acta*, 56(8):3093–3111, 1992. ISSN 00167037. doi: 10.1016/0016-7037(92)90291-P.

Klaas G. J. Nierop, Boris Jansen, and Jacobus M. Verstraten. Dissolved organic matter, aluminium and iron interactions: Precipitation induced by metal/carbon ratio, pH and competition. *Science of the Total Environment*, 300(1-3):201–211, 2002. ISSN 00489697. doi: 10.1016/S0048-9697(02)00254-1.

Jan Nordin, Per Persson, Erkki Laiti, and Staffan Sjöberg. Adsorption of o -Phthalate at the Water−Boehmite (γ-AlOOH) Interface: Evidence for Two Coordination Modes. *Langmuir*, 13(15):4085–4093, 1997. ISSN 0743-7463. doi: 10.1021/la970066g. URL http://pubs.acs.org/doi/abs/10.1021/la970066g.

Jan Nordin, Per Persson, Agneta Nordin, and Staffan Sjöberg. Inner-Sphere and Outer-Sphere Complexation of a Polycarboxylic Acid at the Water−Boehmite (γ-AlOOH) Interface: A Combined Potentiometric and IR Spectroscopic Study. *Langmuir*, 14(13):3655–3662, 1998. ISSN 0743-7463. doi: 10.1021/la9712449. URL http://pubs.acs.org/doi/abs/10.1021/la9712449.

L. O. Öhman, L. Lövgren, T. Hedlund, and S. Sjöberg. The ionic strength dependency of mineral solubility and chemical speciation in solution. In *Surface Complexation Modeling*, chapter 1, pages 1–34. Elsevier, 2006.

Donald A. Palmer and David J. Wesolowski. Aluminum speciation and equilibria in aqueous solution: II. The solubility of gibbsite in acidic sodium chloride solutions from 30 to 70°C. *Geochimica et Cosmochimica Acta*, 56(3):1093–1111, 1992. ISSN 0016-7037. doi: https://doi.org/10.1016/0016-7037(92)90048-N. URL http://www.sciencedirect.com/science/article/pii/001670379290048N.

Johannes Popma. Engineering a horizontal layer of reduced permeability using Al-DOM precipitation. *Delft University of Technology Master Thesis*, 2017.

William Reusch. Acidity of Substituted Phenols, 2014. URL https://chem.libretexts.org/Core/Organic_Chemistry/Phenols/Properties_of_Phenols/Acidity_of_Substituted_Phenols.

David T Richens. *The Chemistry of Aqua Ions: Synthesis, Structure and Reactivity: a tour through the periodic table of the elements*. Wiley, 1997. ISBN 9780471970583. URL https://books.google.nl/books?id=ApwRAQAAIAAJ.

Jörgen Rosenqvist, Kristina Axe, Staffan Sjöberg, and Per Persson. Adsorption of dicarboxylates on nano-sized gibbsite particles: Effects of ligand structure on bonding mechanisms. *Colloids and Surfaces A: Physicochemical and Engineering Aspects*, 220(1-3):91–104, 2003. ISSN 09277757. doi: 10.1016/S0927-7757(03)00063-3.

Daniela Sauer, Herbert Sponagel, Michael Sommer, Luise Giani, Reinhold Jahn, and Karl Stahr. Podzol: Soil of the year 2007. A review on its genesis, occurrence, and functions. *Journal of Plant Nutrition and Soil Science*, 170(5):581–597, 2007. ISSN 14368730. doi: 10.1002/jpln.200700135.

Tatjana Schneckenburger, Jens Riefstahl, and Klaus Fischer. Adsorption of aliphatic polyhydroxy carboxylic acids on gibbsite: pH dependency and importance of adsorbate structure. *Environmental Sciences Europe*, 30(1):1, 2018. ISSN 2190-4707. doi: 10.1186/s12302-017-0129-6. URL https://enveurope.springeropen.com/articles/10.1186/s12302-017-0129-6.

M. Schnitzer and H. Kodama. The dissolution of micas by fulvic acid. *Geoderma*, 15:381–391, 1976.

Garrison Sposito. *The Chemistry of Soils*. Oxford University Press, 2nd edition, 2008. URL https://books.google.nl/books?hl=nl&lr=&id=XCJnDAAAQBAJ&oi=fnd&pg=PR9&dq=The+Chemistry+of+Soils&ots=iGl3g_x17v&sig=IQXWF2G0NIKzTdhLjAUYrp83dTE&redir_esc=y#v=onepage&q=innersphere&f=false.

F. J. Stevenson. *Humus chemistry: genesis, composition, reactions*. J. Wiley & Sons, second edition, 1994. ISBN 0-471-59474-1. URL https://books.google.nl/books?redir_esc=y&hl=nl&id=7kCQch_YKoMC&q=carboxylic+acid#v=onepage&q&f=false.

Werner Stumm and Roland Wollast. Coordination chemistry of weathering: Kinetics of the surface controlled dissolution of oxide minerals, 1990. ISSN 19449208.

Chunming Su and James B. Harsh. Gibbs free energies of formation at 298 K for imogolite and gibbsite from solubility measurements, 1994. ISSN 00167037.

K. H. Tan. The release of silicon, aluminium and potassium during decomposition of soil minerals by humic acid. *Soil Science*, 129(1):5–11, 1980.

Edward Tipping. *Cation Binding by Humic Substances*. Cambridge University Press, Cambridge, 2002. ISBN 9780521621465. doi: DOI:10.1017/CBO9780511535598. URL https://www.cambridge.org/core/books/cation-binding-by-humic-substances/A20E3CC2E78065217DEB8F29E54A4E9E.

H Tipton, J Powell, and Raewyn M Town. Solubility and fractionation of humic acid; effect of pH and ionic medium. *Analytlca Chumca Acta*, 267:47–54, 1992. ISSN 00032670. doi: 10.1016/0003-2670(92)85005-Q.

Venkatesh Uddameri, Sreeram Singaraju, and E. Annette Hernandez. Impacts of sea-level rise and urbanization on groundwater availability and sustainability of coastal communities in semi-arid South Texas. *Environmental Earth Sciences*, 71(6):2503–2515, 2014. ISSN 18666280. doi: 10.1007/s12665-013-2904-z.

Keihei Ueno, Toshiaki Imamura, and K. L. Cheng. *Handbook of Organic Analytical Reagents*. New York, second edition, 1992.

John E. Van Benschoten and James K. Edzwald. Chemical aspects of coagulation using aluminum salts - I. Hydrolytic reactions of alum and polyaluminum chloride. *Water Research*, 24(12):1519–1526, 1990. ISSN 00431354. doi: 10.1016/0043-1354(90)90086-L.

P. A.W. Van Hees, Ulla S. Lundström, and R Giesler. Low molecular weight organic acids and their Al-complexes in soil solution - Composition, distribution and seasonal variation in three podzolized soils. *Geoderma*, 94(2-4):173–200, feb 2000. ISSN 00167061. doi: 10.1016/S0016-7061(98)00140-2.

P. A.W. Van Hees, S. I. Vinogradoff, A. C. Edwards, D. L. Godbold, and D. L. Jones. Low molecular weight organic acid adsorption in forest soils: Effects on soil solution concentrations and biodegradation rates. *Soil Biology and Biochemistry*, 35(8):1015–1026, 2003. ISSN 00380717. doi: 10.1016/S0038-0717(03)00144-5.

Andre van Zomeren. *On the nature of organic matter from natural and contaminated materials*. 2008. ISBN 9789085049937.

J. Verbruggen, A. Moermond, A. Janus, and A. Lijzen. *Afleiding van milieurisicogrenzen voor chloride in oppervlaktewater , grondwater , bodem en waterbodem Afleiding van milieurisicogrenzen voor chloride in oppervlaktewater , grondwater , bodem en waterbodem*. 2008. ISBN 0302749101.

Remco Vis. Control of Subsurface Flow The Effect of Al-OM Interactions on Hydraulic Conductivity. *Delft University of Technology Master Thesis*, (August), 2015.

Shin-Ichiro Wada and Yasuko Kakuto. Solubility and standard Gibbs free energy of formation of natural imogolite at 25°c and 1 atm. *Soil Science and Plant Nutrition*, 45(4):947–953, 1999. doi: 10.1080/00380768.1999.10414344. URL https://doi.org/10.1080/00380768.1999.10414344.

Sarah H. Wallace, Samuel Shaw, Katherine Morris, Joe S. Small, Adam J. Fuller, and Ian T. Burke. Effect of groundwater pH and ionic strength on strontium sorption in aquifer sediments: Implications for90Sr mobility at contaminated nuclear sites. *Applied Geochemistry*, 27(8):1482–1491, 2012. ISSN 08832927. doi: 10.1016/j.apgeochem.2012.04.007. URL http://dx.doi.org/10.1016/j.apgeochem.2012.04.007.

Karl Wefers and Chanakya Misra. Oxides and Hydroxides of Aluminum. *Alcoa Technical Paper*, 19: 1–100, 1987.

L.P. Weng. *Interactions between metal ions and biogeo-surfaces in soil and water*. PhD thesis, Wageningen University, 2002.

David J. Wesolowski. Aluminum speciation and equilibria in aqueous solution: I. The solubility of gibbsite in the system Na-K-Cl-OH-Al(OH)4from 0 to 100°C. *Geochimica et Cosmochimica Acta*, 56 (3):1065–1091, 1992. ISSN 00167037. doi: 10.1016/0016-7037(92)90047-M.

David J. Wesolowski and Donald A. Palmer. Aluminum speciation and equilibria in aqueous solution: V. Gibbsite solubility at 50°C and pH 3-9 in 0.1 molal NaCl solutions (a general model for aluminum speciation; analytical methods). *Geochimica et Cosmochimica Acta*, 58(14):2947–2969, 1994. ISSN 00167037. doi: 10.1016/0016-7037(94)90171-6.

Feng Xiao, Baojie Zhang, and Chery Lee. Effects of low temperature on aluminum(III) hydrolysis: Theoretical and experimental studies. *Journal of Environmental Sciences*, 20(8):907–914, 2008. ISSN 1001-0742. doi: https://doi.org/10.1016/S1001-0742(08)62185-3. URL http://www.sciencedirect.com/science/article/pii/S1001074208621853.

Z. Xu. General report Geotechnical problems of dikes (TC 201) and dams (TC 210) Rapport général. (Tc 201):3281–3287, 2013.

Hui Bin Yang, Xiao Lin Pan, Hai Yan Yu, Gan Feng Tu, and Jun Min Sun. Dissolution kinetics and mechanism of gibbsitic bauxite and pure gibbsite in sodium hydroxide solution under atmospheric pressure, 2015. ISSN 10036326.

Raymond Nen Yong and Frank C. Townsend. *Consolidation of Soils: Testing and Evaluation*. ASTM International, 1986. ISBN 978-0-8031-0446-4. URL https://books.google.com/books?id=a-BKqGTXA6kC.

Haoyu Zhang. Rapid determination of dissolved organic carbon by persulfate oxidation vial and UV/VIS spectrophotometer. *Environmental Engineering*, 2013.

Ádám Zsolnay. Dissolved organic matter: Artefacts, definitions, and functions. In *Geoderma*, volume 113, pages 187–209, 2003. ISBN 0016-7061. doi: 10.1016/S0016-7061(02)00361-0.

A

Podzolization

Already in 1856 Barth presented a detailed description of a podzol, which he named lead sand (Lundström et al., 2000a). Since then a lot of research has been done on podzolization, leading to multiple (partly conflicting) podzolization theories.

None the less an attempt was made to summarize the podzolization process into four steps:

1. Dissolution of Al and Fe containing minerals
2. Downward transport of Al and Fe
3. Immobilization of Al and Fe
4. Precipitation of Al and Fe complexes

1. Dissolution There is an overwhelming evidence that DOM promotes the dissolution of minerals by complexing with Al and Fe (Kodama et al., 1983; Schnitzer and Kodama, 1976; Tan, 1980). LMW acid complex best, Lundström et al. (2000b) stated that mineral dissolution via complexing LMW acids is a major weathering process in podzols.

2. Downward transport Considering the abundant evidence of the complexing ability of DOM with Al and Fe (Van Hees et al., 2003) together with the demonstrated ability of these acids to promote dissolution of minerals. It has been generally accepted that Al and Fe migrate downwards from the E to the B horizon in the form of organic complexes (Buurman and Jongmans, 2005; Lundström et al., 2000b,a).

3. Immobilization Where there is a general consensus on the mechanism controlling the downward transport two main theories considering the mechanism of immobilization do now prevail (Lundström et al., 2000b).

Adsorption theory
Unsaturated soluble metal-organic complexes are transported downward and immobilized (and subsequently precipitated) in the B horizon upon saturation of organic molecules through further complexation (McKeague et al., 1978). Complexation is mainly attributed to FA and HA.

Biodegradation theory
In this theory the complexation and subsequent downward transport is mainly attributed to LMW acids. These ‘carriers’ are microbially broken down, releasing Al and Fe (Lundström et al., 2000b; Van Hees et al., 2000).

4. Precipitation In the adsorption theory saturated metal-organic complexes are immobilized by precipitation. Continuing addition of metals during the downward migration until a certain C/M ratio has been reached, caused the complex to precipitate. In the biodegradation theory Al and Fe are released by microbial degradation of LMW acid metal complexes. The released Al and Fe complex with HMW acids and precipitate or precipitate as inorganic phase and adsorb HMW acids to their surfaces (Lundström et al., 2000b).

As stated earlier many (partly conflicting) podzolization theories exist. With now a general consensus on the dissolution and downward transport. But the mechanisms of immobilization and precipitation are still debated. For example Sauer et al. (2007) suggested in total eight mechanisms of immobilization and stated that multiple mechanisms might be involved at the same time. (Jansen et al., 2005) found no evidence of immobilization due to microbial degradation. They however state that different podzolization mechanisms dominate under different conditions, explaining the discrepancies in literature.

B

Second experiment series

All samples were created on 15-02-18 and on the same day samples E2.1Sz with z = 1-5, were acidified. All other sample were acidified on 16-02-18. Four extra samples were (re)created (E2.1S4 -3, E2.1S4 -4 , E2.1S7 -3 and E2.3S4.5 -2) because the original samples pH deviated 0.2 or more from their target pH.

Sample	pH_{target}	$pH_{initial}$	1.6M HCL (mL)	0.1M HCL (mL)	pH	EC (μs/cm)
E2.1S2	2	9.14	0.440		2.00	7830
E2.1S2 -2	2	9.17	0.440		1.98	7950
E2.1S2.5	2.5	9.17	0.230		2.45	3230
E2.1S3	3	9.15	0.160		3.02	1772
E2.1S3 -2	3	9.20	0.160		2.99	1677
E2.1S3.5	3.5	9.15	0.130		3.60	1466
E2.1S4	4	9.14	0.140		3.30	1566
E2.1S4 -2	4	9.18	0.130		3.67	1273
E2.1S4 -3	4	8.97	0.116		3.75	1224
E2.1S4 -4	4	8.96	0.109		4.07	1165
E2.1S4.5	4.5	9.05	0.100		4.50	1240
E2.1S5	5	8.99	0.082	0.165	4.02	1172
E2.1S5 -2	5	9.03	0.870		4.76	1068
E2.1S5 -3	5	8.94	0.084		4.82	1062
E2.1S6	6	9.00	0.040	0.200	6.02	1061
E2.1S7	7	8.97		0.435	7.02	971
E2.1S7 -2	7	8.99		0.430	7.00	862
E2.1S8	8	8.96		0.200	8.02	935

Sample	pH_{target}	$pH_{initial}$	1.6M (mL)	HCL	0.1M (mL)	HCL	pH	EC (μs/cm)
E2.2S2	2	9.00	0.425				1.99	7770
E2.2S2 -2	2	9.04	0.425				1.98	7960
E2.2S2.5	2.5	9.03	0.200				2.53	2630
E2.2S3	3	9.04	0.140				3.08	1524
E2.2S3 -2	3	9.04	0.145				2.99	1535
E2.2S3.5	3.5	9.02	0.115				3.53	1277
E2.2S4	4	9.02	0.105				3.98	1180
E2.2S4 -2	4	9.00	0.105				3.95	1138
E2.2S4.5	4.5	8.99	0.085				4.45	1102
E2.2S5	5	8.98	0.050		0.540		4.84	1034
E2.2S5 -2	5	8.96	0.060		0.300		5.00	988
E2.2S6	6	8.94	0.043				6.06	917
E2.2S7	7	8.93			0.360		7.08	840
E2.2S7 -2	7	8.95			0.402		7.01	816
E2.2S8	8	8.92			0.160		8.10	809

Sample	pH_{target}	$pH_{initial}$	1.6M (mL)	HCL	0.1M (mL)	HCL	pH	EC (μs/cm)
E2.3S2	2	8.50	0.244				2.04	4340
E2.3S2 -2	2	8.67	0.262				2.04	4680
E2.3S2.5	2.5	8.75	0.130		0.150		2.52	1832
E2.3S3	3	8.73	0.095		0.150		3.03	1191
E2.3S3 -2	3	8.68	0.102		0.080		2.99	1203
E2.3S3.5	3.5	8.68	0.082		0.082		3.56	993
E2.3S4	4	8.69	0.070		0.175		4.03	901
E2.3S4 -2	4	8.64	0.076				4.01	913
E2.3S4.5	4.5	8.65	0.070				4.29	874
E2.3S4.5 -2	4.5	8.59	0.064				4.52	868
E2.3S5	5	8.68	0.054				5.07	802
E2.3S5 -2	5	8.67	0.055				4.99	810
E2.3S6	6	8.65			0.600		6.05	718
E2.3S7	7	8.64			0.235		7.01	674
E2.3S7 -2	7	8.63			0.250		6.90	675
E2.3S8	8	8.63			0.075		8.03	648

C

Data on electric conductivity (EC)

C.1. Experiments series one

During the first series of experiments a sudden EC drop was measured at high EC levels after the same date, presumably due to contamination of the 0.1M KCL calibration buffer.

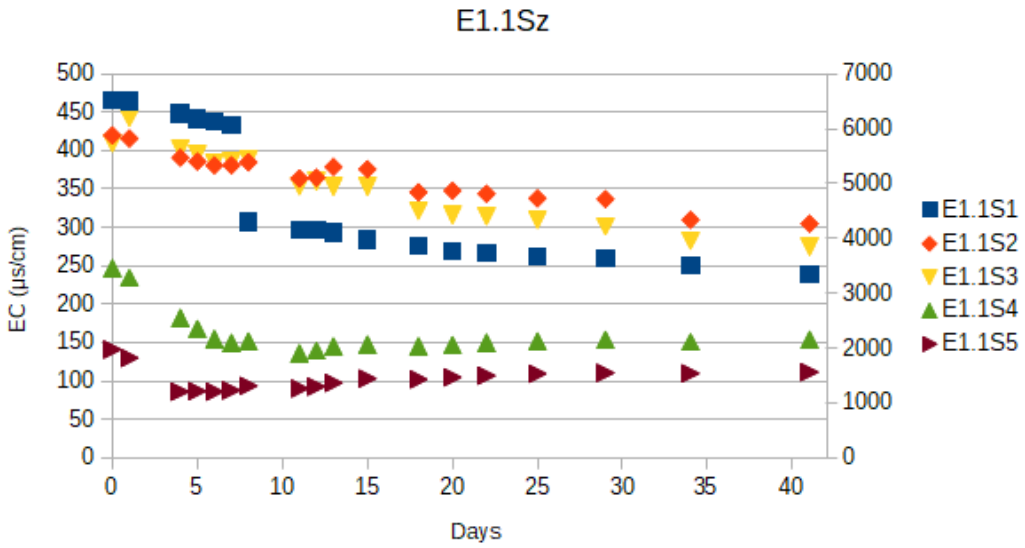

Figure C.1: EC measurements E1.1Sz

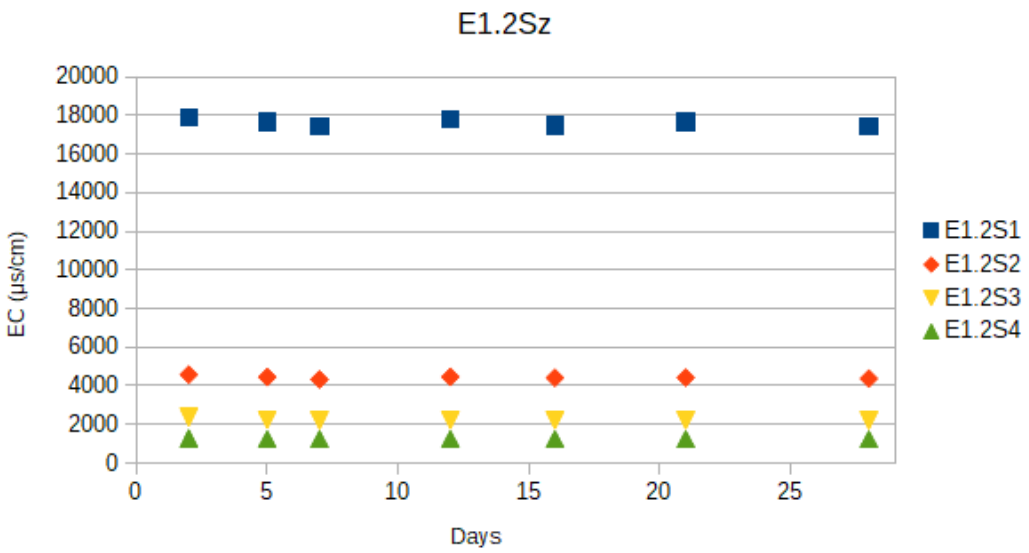

Figure C.2: EC measurements E1.2Sz

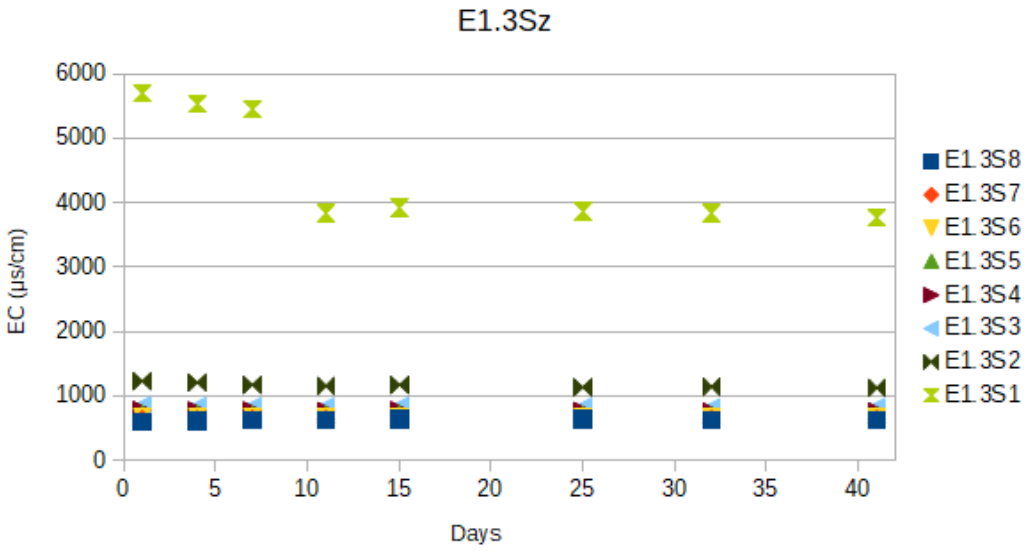

Figure C.3: EC measurements E1.3Sz

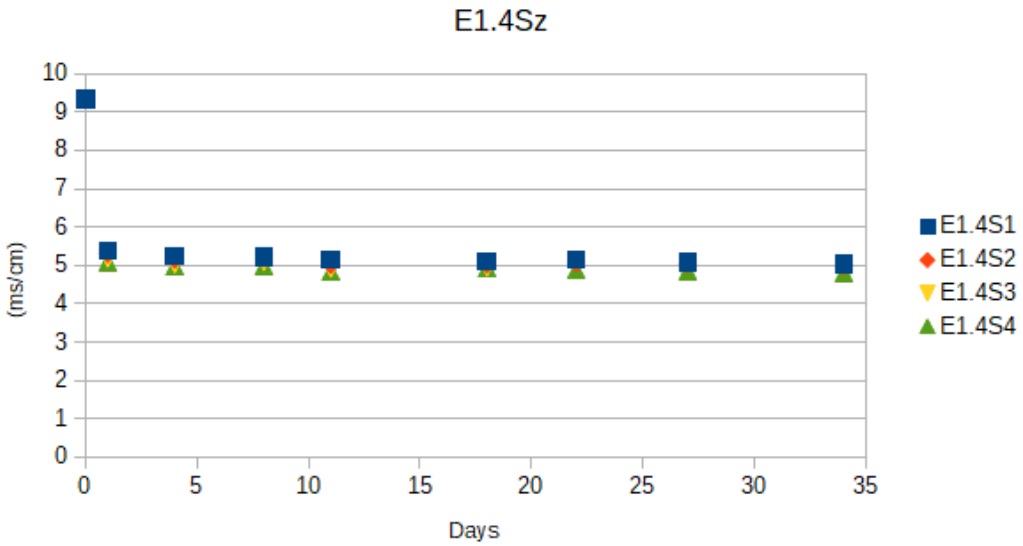

Figure C.4: EC measurements E1.4Sz

C.2. Experiments series two

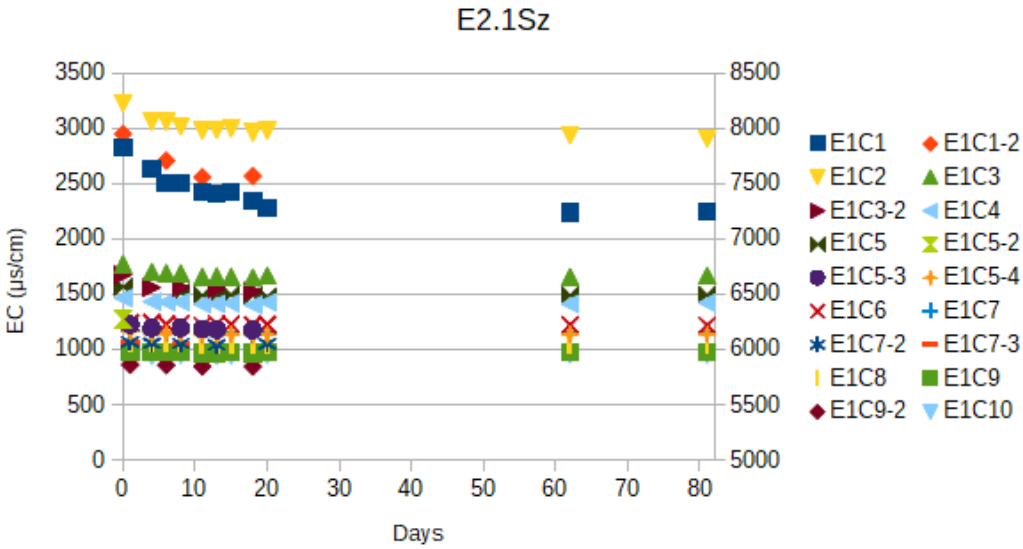

Figure C.5: EC measurements E2.1Sz

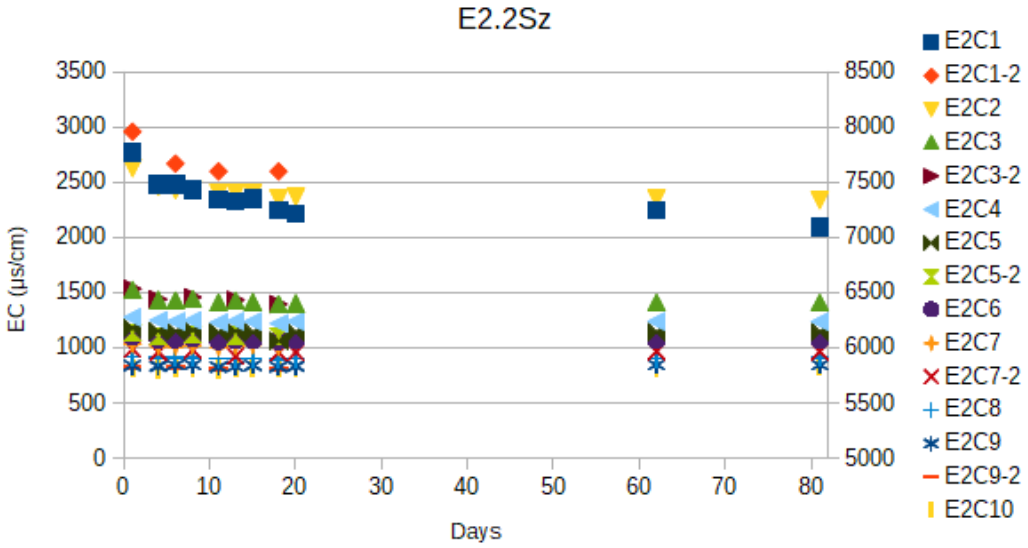

Figure C.6: EC measurements E2.2Sz

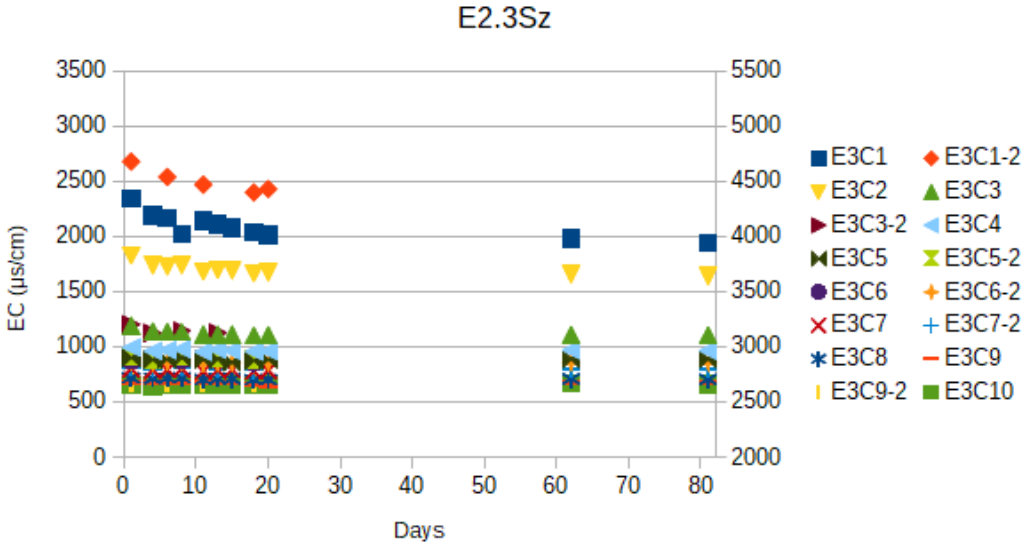

Figure C.7: EC measurements E2.3Sz

D

Al measurements

The aluminum measurements done on E2.2Sz and E2.3Sz at the starting pH range 2 - 3.5 are given in the figure D.1. The data could not be fully explained.

In Hach (2017) the recommended conditions (pH and temperature) and interference levels of ions are given. The recommendation on sample pH: 2.5 - 3.5 and temperature: 20-23 degrees were met. And the interference levels of K^+ and Cl^- were not exceeded.

At starting pH = 2 ; 2.5 ; 3 a trend of higher aluminum concentration at lower pH can be seen. Agreeing with what is expected from the pH dependend dissolution of gibbsite. Measurements at starting pH = 3.5 do not comply with this trend. At starting pH = 2 ; 2.5 ; 3 most of the HUMIN precipitated (at the end of the experiment) and a small fraction stayed soluble (see figures 4.8,4.9 and 4.11) whereas at starting pH = 3.5 most of the HUMIN stayed soluble (see figure 4.12). Indicating that the higher DOM concentration interfered with the measurements or enhanced the gibbsite dissolution.

Another visible trend is the Al concentration difference between E2.2Sz (depicted in red) and E2.3Sz (depicted in blue). The difference in the amount of gibbsite cannot be the cause of this trend, as a higher or at least equal Al concentration is expected from the fact that E2.3Sz has a higher amount of gibbsite than E2.2Sz. The sampling for the Al measurements was done just below the samples surface, from the supernatent. The difference in Al concentration can therefore only be explained by the DOM concentration.

The DOM has deprotonated functional groups available for binding with Al^{3+}, which has a higher affinity to these functional groups than H^+. Because E2.2S2.5 has a higher HUMIN starting concentration then E2.3S2.5, accordingly the remaining DOM concentration after the self-flocculation is also higher. This means that there are more binding sites for Al. Because the Al/C ratio is very low the Al^{3+} and DOM for soluble complexes.

From Hach (2013) it was concluded that the Al kit measured free Al only. But the reactive substance, chromazurol S, is a organic reagent that by complexation with free AL creates a coloured solution. At the recomended pH range chromazurol S forms single bonds with Al (Ueno et al., 1992). It is therefore possible that soluble unsaturated Al-DOM complexes complex with chromazural. Furthermore it is not far-fetched that it is possible that chromazural S is able to 'steal' Al from soluble Al-DOM complexes. In both cases this means that the kit doesn't measure the free Al but (some) of the Al bounded to DOM as well.

The formation of more soluble complexes at higher DOM concetration in combination with the potential of the measuring kit to measure bounded Al can explain the Al concentration difference between E2.2Sz and E2.3Sz. But could also have interferred with the UV measurements. As was also suggested by the non-compliance of the measurements at starting pH = 3.5 with the pH dependend dissolution of gibbsite. The HUMIN was assumed not to significantly interfere at 620 nm but probably has. Both

processes of partly measuring bounded Al and the interference of DOM are likely the cause of the difficulty to explain the Al measurements. At this point it is not possible to atributed relative importance to both processes.
There might also be unknown reactions of HUMIN within the measuring kit. More extensive UV measurements on HUMIN at 620 nm in combination with measurements with known Al^{3+} and HUMIN concentration could help validate whether the Al measurements conducted in this study are reliable or could be calibrated.

Lastly a trend of constant Al concentration over time is noteable. Likely a intermediate equilibrium has been reached between the dissolution and (soluble) Al-DOM complex formation. Another hypothesis is opted but in all probability not significant. Overal the HUMIN protonated and subsequently precipitated fast, indicating that relatively large and dense flocs were formed. In these relatively large flocs, deprotonated functional groups are present. These groups are unable to protonate because the intertwined HUMIN molecules pose an energy barrier. But Al^{3+} electrostatically has an higher affinity to bind to DOM's functional groups and is therefore able to overcome this energy barrier. The dissolution and complexation seen from the Al measurements took place during acidification, when DOM hadn't precipitated and covered the gibbsite yet. While the Al from the continuous dissolution of gibbsite was captured by the precipitated DOM and therefore not seen in the Al measurements.

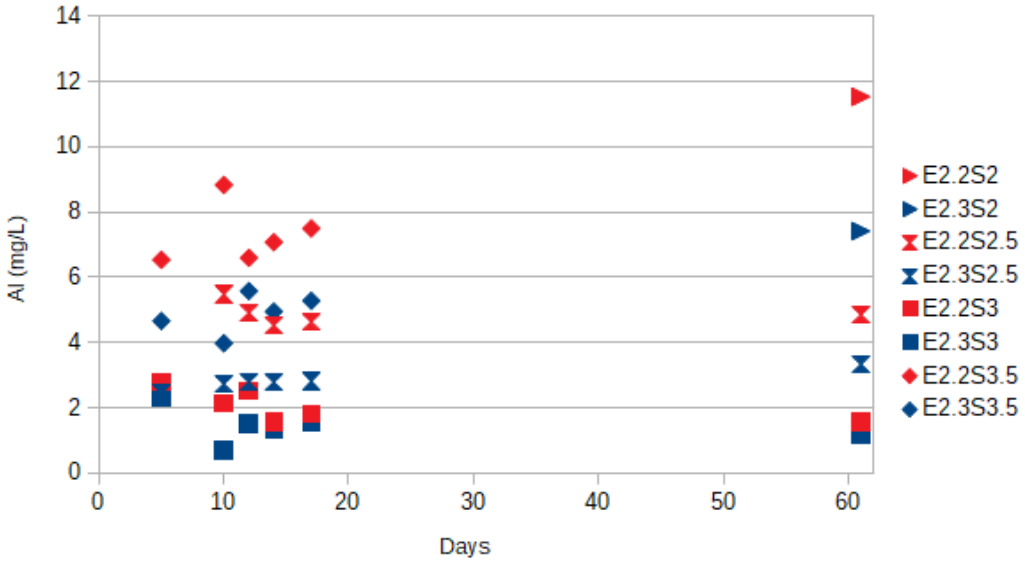

Figure D.1: Al measurements E2.2Sz and E2.3Sz at starting pH = 2 - 3.5

E

DOM results E2.2Sz at high pH

Table E.1: Starting pH, final pH with the experimental duration, HUMIN concentration and amount of gibbsite of E2.2Sz at high pH

	pH_{start}	pH_{final} (days)	$\Delta[H^+](mmol/L)$	HUMIN (g/L)	Gibbsite (g/L)
E2.2S4	3.98	4.67 (61)	-0.08	2.7	0.35
E2.2S4.5	4.45	5.23 (61)	-0.03	2.7	0.35
E2.2S5 -2	5.00	5.84 (61)	-0.01	2.7	0.35
E2.2S6	6.06	7.27 (61)	-0.00	2.7	0.35
E2.2S7	7.08	7.77 (61)	-0.00	2.7	0.35
E2.2S8	8.10	7.95 (61)	0.00	2.7	0.35

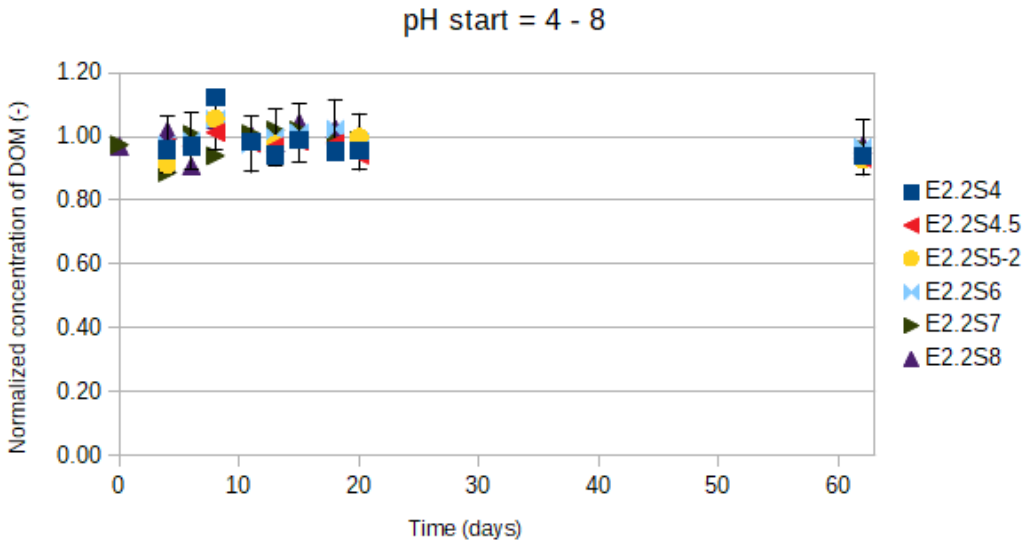

Figure E.1: DOM concentration normalized to the initial DOM concentration (t_0) of E2.2Sz over time.

F

DOM results E2.3Sz at high pH

Table F.1: Starting pH, final pH with the experimental duration, HUMIN concentration and amount of gibbsite of E2.3Sz at high pH

	pH_{start}	pH_{final} (days)	$\Delta[H^+](mmol/L)$	HUMIN (g/L)	Gibbsite (g/L)
E2.3S4	4.03	4.85 (61)	-0.08	1.9	1.45
E2.3S4.5 -2	4.52	5.40 (61)	-0.03	1.9	1.46
E2.3S5 -2	4.99	5.98 (61)	-0.01	1.9	1.46
E2.3S6	6.05	7.32 (61)	-0.00	1.9	1.43
E2.3S7	7.01	7.74 (61)	-0.00	1.9	1.45
E2.3S8	8.03	7.88 (61)	0.00	1.9	1.46

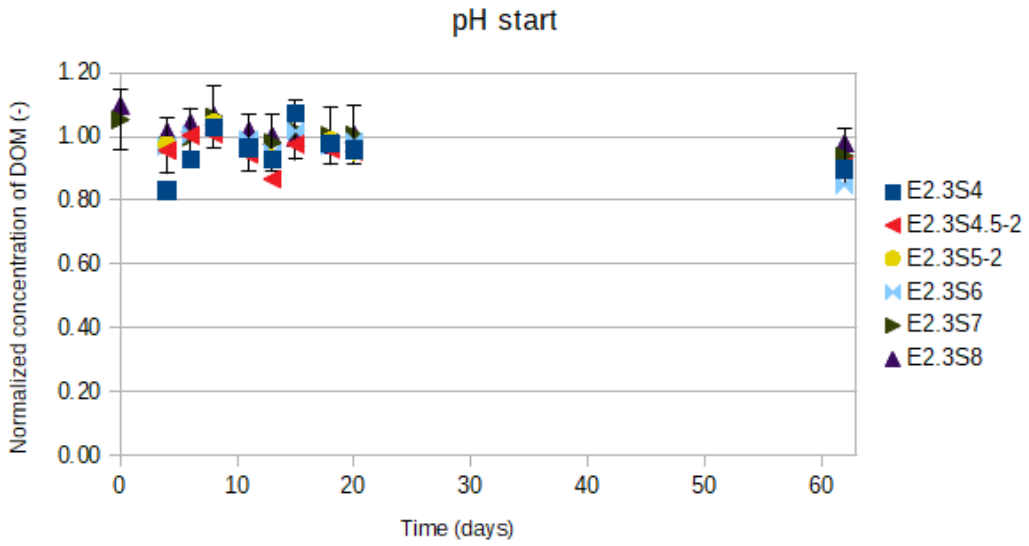

Figure F.1: DOM concentration normalized to the initial DOM concentration (t_0) of E2.3Sz over time.